

W-32  
NATIONAL ADVISORY COMMITTEE FOR AERONAUTICS

JPL LIBRARY

CALIFORNIA INSTITUTE OF TECHNOLOGY

# WARTIME REPORT

ORIGINALLY ISSUED

January 1943 as  
Advance Restricted Report

THE SIGNIFICANCE OF THE TIME CONCEPT IN ENGINE DETONATION

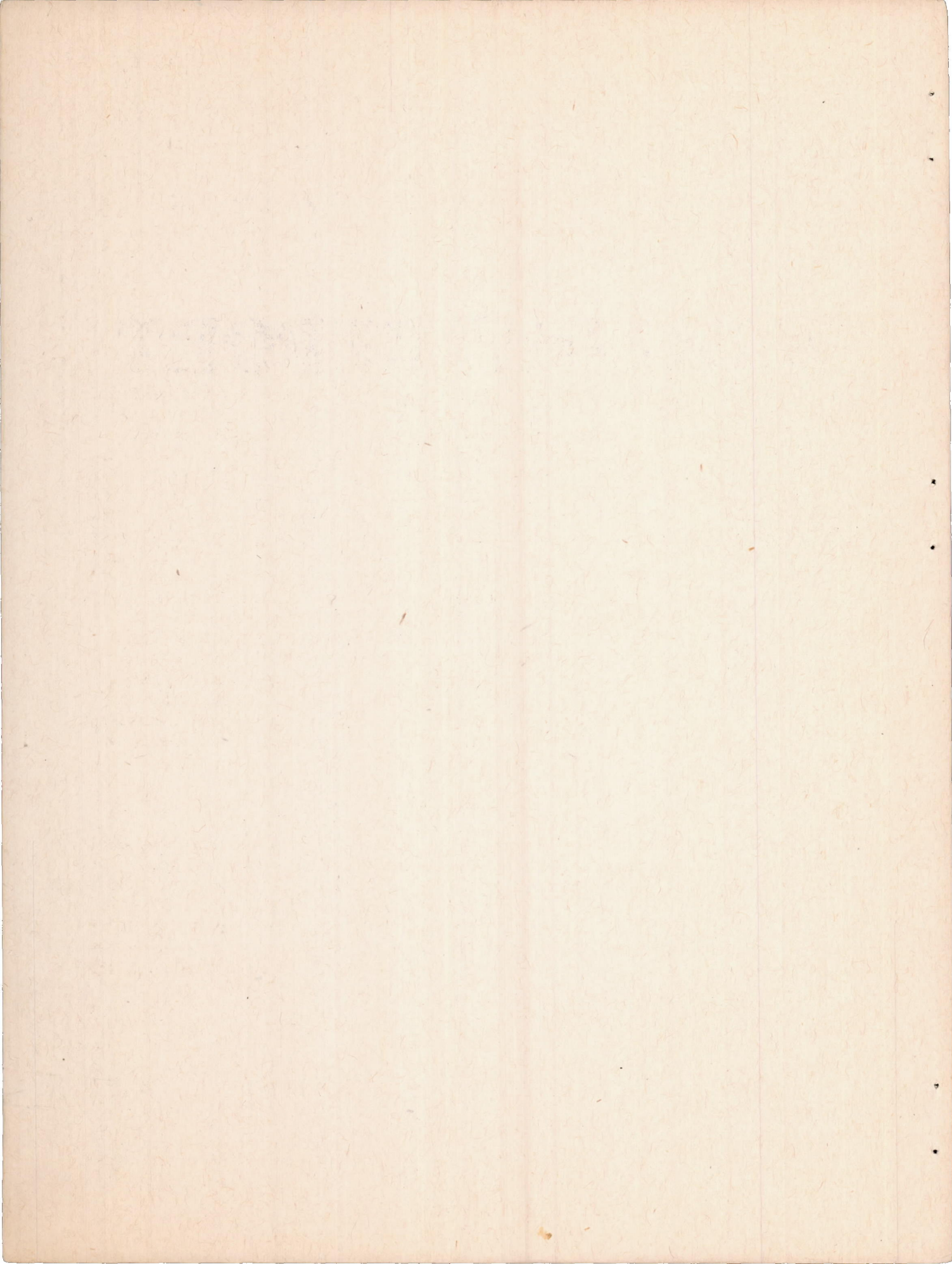
By W. A. Leary and E. S. Taylor  
Massachusetts Institute of Technology



WASHINGTON

NACA WARTIME REPORTS are reprints of papers originally issued to provide rapid distribution of advance research results to an authorized group requiring them for the war effort. They were previously held under a security status but are now unclassified. Some of these reports were not technically edited. All have been reproduced without change in order to expedite general distribution.







# NATIONAL ADVISORY COMMITTEE FOR AERONAUTICS

## ADVANCE RESTRICTED REPORT

### THE SIGNIFICANCE OF THE TIME CONCEPT IN ENGINE DETONATION

By W. A. Leary and E. S. Taylor

#### SUMMARY

An experimental technique has been developed by means of which the variables affecting the time element in the detonation process in a spark-ignition engine can be controlled and approximately measured. It is shown that increasing the rate of compression of the unburned charge allows higher peak pressures to be used. The importance of the ignition delay is demonstrated by observing that pressure and temperature considerations are insufficient to describe completely the events leading to detonation. The effect of variation in the time element on the maximum permissible pressure, the temperature, and the relative density of the last part of the charge to burn has been determined. Certain aspects of ignition delay and the mechanism of normal and detonating combustion are discussed on the basis of chain-reaction theory. Suggestions are offered for a more satisfactory basis of comparison for detonation data. A discussion of the precision of various methods of determining the pressure and temperature of the unburned charge is included. On the basis of information and experience gained in this investigation, a new and simplified experimental approach to the detonation problem is outlined.

#### INTRODUCTION

The fact that detonation, or knocking, in the gasoline engine is a function of more than a dozen operating variables and occurs with explosive rapidity explains why the development of a consistent theory has been such a long and tedious process. Fifteen years ago there were at least eight more or less plausible explanations of the phenomenon (reference 1). The existence of so many hypotheses was a direct consequence of the difficulty of observing what was actually happening inside the engine cylinder and measuring the effects.



The first of these difficulties was overcome in 1931 when Withrow and Boyd (reference 2) succeeded in photographing the process of combustion in an actual engine. This technique was extended by Withrow and Rassweiler (reference 3) to include photographic studies of detonating combustion. These photographs showed that detonation was the result of a reaction which took place in the unburned charge ahead of the normal flame front and was not, as had been supposed by some, an extremely rapid acceleration of the normal flame in the later stages of combustion.

Attention was then focused on the autoignition hypothesis of detonation. This hypothesis was first advanced by Ricardo (reference 4), who suggested that detonation might be spontaneous ignition of the unburned part of the charge ahead of the normal flame front. This explanation failed to show why kerosene, with a higher ignition temperature than carbon disulfide, detonated more readily in a given engine. A satisfactory explanation of this apparent contradiction was presented in 1935 by one of the authors (reference 5) who, basing his reasoning largely on the experimental work of Tizard and Pye (reference 6), showed that no contradiction need exist if it is assumed that detonation will occur only when the unburned part of the charge is heated to, or above, its ignition temperature and held there for a definite length of time. This time interval is known as the ignition delay.

The autoignition hypothesis is a purely physical interpretation of detonation and has the saving grace of simplicity. Through its use detonation may be thought of, not as a function of a dozen or more engine conditions, but rather in terms of the three fundamental variables: pressure, temperature, and time. This hypothesis is perhaps the one most generally accepted at the present time. The difficulty of checking it quantitatively still involves the problem of accurate measurements; although the task is not so formidable as when the hypothesis was first advanced. The development of the high-speed engine indicator, the cathode-ray oscillograph, and high-speed photographic and stroboscopic technique, as well as the availability of more homogeneous fuels, has brought verification of the hypothesis within the scope of refined experimental technique.

The rapidly varying pressures in a high-speed engine cylinder now can be measured with fair accuracy. There is no means now available, however, for measuring directly the rapidly varying temperature of the unburned part of the charge and hence this



fundamental variable can, at present, be investigated only by means of thermodynamic laws. An investigation of the precision of this method, given in appendix A, indicates that the temperature so determined should be reasonably close to the true value.

At the present writing, the effect of end gas (the part of the charge ahead of the flame front), temperature, and pressure on detonation has been investigated experimentally by Serruys (reference 7), Rothrock and Biermann (reference 8), and the authors and Diver (reference 9). The third basic variable, time, which is the most elusive aspect of the problem, is the subject of the present report. The problem to be discussed is complicated by four distinct effects:

1. The time during which heat is transferred to or from the unburned charge
2. The speed at which the normal flame traverses the combustion chamber
3. The motion of the piston
4. The ignition delay

It is generally recognized that the first three of the effects listed influence engine detonation either directly or indirectly to a large extent, but the significance of the fourth effect is often questioned. The effect of many engine variables on detonation - fuel-air ratio, for instance - can be determined experimentally without recognizing that delay exists (reference 9). Here the analysis can be treated solely by means of temperature-pressure considerations. This treatment has been in general use in the past, and, as a result, the delay has been assumed by some to have negligible influence. It is shown in this report, however, that large changes in end-gas pressure, temperature, and density for a given level of detonation cannot be accounted for without the supposition of an ignition delay.

The chief challenge to the autoignition hypothesis comes from recent work (references 10, 11, and 12). This work is based on schlieren photographs and motion pictures of the combustion process in a special cylinder. The photographs of references 11 and 12 were taken at the rate of 40,000 frames per second. These photographs have been interpreted to indicate that detonation may occur only after the entire charge has been inflamed, either by



passage of the flame front or by autoignition. The authors of the present paper believe that this interpretation may prove eventually to be erroneous, for reasons explained in appendix B. In case, however, it is finally established that the flame does indeed pass completely through the charge before detonation, the autoignition hypothesis may have to be modified. For the present, the authors of this report prefer to retain the autoignition hypothesis for the following reasons:

- (a) The autoignition hypothesis fits all known observations with regard to detonation in an actual engine.
- (b) The autoignition hypothesis furnishes a simple and convincing explanation of the experimental facts revealed in the present report.
- (c) If, at a later date, the autoignition theory should be definitely disproved, the basic conclusion arrived at in this report - namely, that there is an important time effect connected with the process of detonation - would not be affected.

The authors wish to acknowledge their appreciation for the assistance rendered by Professor C. F. Taylor in suggesting helpful experimental approaches to the problem and for his invaluable criticism of the manuscript. The authors are also indebted to Professor A. R. Rogowski, J. R. Diver, and J. E. Forbes of the Sloan Laboratory staff for their kind assistance during the experimental tests. The suggestions of the NACA technical staff were also of considerable assistance in preparing the manuscript.

#### DESCRIPTION OF APPARATUS

A photograph and a schematic diagram of the apparatus are shown in figures 1 and 2. The apparatus was the same as that used at the Massachusetts Institute of Technology in an earlier investigation of detonation (reference 9), except as follows:

The engine was a new CFR engine with high-speed camshaft and aluminum piston but without the reciprocating balancing weights usually supplied. These weights were unnecessary because the engine was bolted to a 9.5-ton bed plate mounted on rubber



vibration isolators. The engine was originally equipped with a standard high-speed inlet valve, but with this valve detonation was very nonuniform at all speeds. A shrouded inlet valve was then installed and excellent uniformity was obtained. This uniformity seemed to be at its best when the engine speed was about 1200 rpm and the spark advance about 30° B.T.C. Inlet temperature had no apparent effect on uniformity in the range from 120° F to 200° F.

The evaporative cooling system was augmented by an electrically driven circulator pump in order to obtain a more uniform temperature distribution throughout the cylinder jacket. Fuel was delivered to a vaporizing tank of about 15 gallons capacity by a new high-speed Bosch fuel pump, having a 7-millimeter plunger. An exhaust surge tank of about 8.5 gallons capacity was used.

The exact engine speed was conveniently identified by painting 36 equally spaced radial lines on the rim of the flywheel and illuminating it with a strobotac operating on 60-cycle frequency. At multiples of 100 rpm the pattern appeared stationary, showing the marks clearly; while at multiples of 50 rpm the stationary effect was obtained with 72 marks showing. Best performance was obtained at 800 rpm with a Champion spark plug No. 8 CFR and at 1600 and 2400 rpm with a BG 3B2 spark plug.

The runs being made during hot weather, the entire fuel system was kept under a gage pressure of about 24 pounds per square inch. This precaution insured freedom from vapor-lock troubles and made operation of the fuel pump reliable.

Fuel measurements were made by weighing a definite amount of fuel with a sensitive balance. The balance was so arranged that it operated an electric relay which actuated an electric clock and an electric counter on the air meter. The sensitivity of the balance was about 1 part in 2000. With this device fuel-air ratios could be accurately determined without personal errors. A rotameter was used as a check on the constancy of fuel flow. A diagram of the fuel system is shown in figure 3 and a complete description of the system is given in appendix C.

An electrically driven Roots blower was used to supply the additional boost needed at high speeds. A Ford Model A radiator immersed in a tank of running water proved very satisfactory as an intercooler. The temperature variation of the air leaving the intercooler did not vary by more than 2° F in any given series of runs regardless of the boost pressure.



The fuel-air mixing valve (see reference 9, fig. 6) was modified by changing the size of the mixing orifice from  $1/2$  to  $7/8$  inch so as not to cause unnecessary restriction at high speed and it was then found to work satisfactorily at all speeds.

As far as practicable, rubber hose and flexible joints were avoided in the inlet system between the air meter and the engine. Connections were made rigid and airtight either with threaded pipe fittings or flanges and gaskets. The connection between the vaporizing tank and the engine was a piece of flanged brass pipe. This arrangement made it necessary that the tank be free to move up and down with the cylinder head as the compression ratio was varied. The tank was therefore mounted on springs and was so adjusted that no load was on the inlet pipe at the mean position of the cylinder head. It was also necessary to support the heater and the drying tower on springs because they were rigidly connected to each other and to the vaporizing tank.

#### EXPERIMENTAL PROCEDURE

The experimental program was designed to provide a means of demonstrating, for the case of incipient detonation, the effect of changes in the rate of compression of the unburned charge on its maximum permissible pressure. In this work maximum permissible pressure was defined as the pressure of the unburned part of the charge at the instant when incipient detonation occurs. In most of the runs maximum permissible pressure was coincident with peak pressure, but in some cases, especially where combustion was completed before top center, maximum permissible pressure was lower than peak pressure, also, it was assumed that the pressure of the unburned charge from inlet-valve closing to the instant of detonation was the pressure given by the indicator diagram.

The pressure-time curve was of particular importance in this investigation. By a comparison of pressure-time paths associated with constant incipient detonation under various engine operating conditions, the relation between ignition delay and rate of compression can be established. The experimental work therefore was arranged to give indicator diagrams of various shapes under rigidly controlled operating conditions.

The shape of the compression path can be altered by changing operating variables, such as inlet pressure, engine speed, fuel-air ratio, and so forth; but, in order to study time effects, it



was found desirable to change the shape by varying only spark advance and compression ratio at a given engine speed. A change in spark advance causes peak pressure to occur earlier or later in the cycle (see figs. 4, 5, and 6) and results in a change in detonation intensity. If the compression ratio is adjusted to give the original intensity of detonation, it can be stated that the permissible change in compression ratio (or maximum pressure) is associated with the change in the path of compression.

Runs were made with varying spark advance at three different (constant) engine speeds. In each run, compression ratio was adjusted to give incipient detonation. The variables held constant for all runs were: air consumption per cycle, fuel consumption per cycle, inlet-air humidity, and coolant temperatures. The engine was warmed up for about two hours before making runs, during which time the inlet pressure was varied by trial to give the correct air consumption, the fuel-air ratio was adjusted, and temperature equilibrium was established. Incipient detonation was identified by observing the  $dp/dt$  (rate of change of pressure) trace on a cathode-ray oscillograph with the same apparatus and by the same method used in reference 9.

Air consumption was maintained at 0.000932 pound of dry air per cycle either by throttling or by supercharging. The variation from this value in 98 percent of the runs was less than 1 percent and the maximum variation was 2.5 percent. The residual gas content varied from 4 to 7.5 percent. The total weight of charge (air + fuel + residual gas) per cycle was maintained at  $0.001065 \pm 0.000025$  pound or a maximum variation of less than 2.5 percent for all runs; although the maximum variation in this quantity for runs selected for analysis was less than 2 percent. The fuel-air ratio was maintained at 0.0789 with a variation of less than 1 percent in 96 percent of the runs and a maximum variation of 2.2 percent. Engine speed was maintained within 2 rpm of the desired value, and inlet temperatures were held to within  $1^{\circ}$  F. The effect of atmospheric humidity was eliminated by the use of a drying tower using activated alumina. (See appendix A of reference 9.) Checks on the dew point of the inlet air were made for each run and, although this value was probably in the neighborhood of  $-60^{\circ}$  F, no attempt was made to determine it precisely. As long as the dew point was below  $-40^{\circ}$  F, it was considered satisfactory, since a dew point of  $-40^{\circ}$  F corresponds to a water-vapor content of about 1 percent of the water vapor in the residual gases. The coolant temperature was maintained at  $212^{\circ}$  F.



When operating conditions were brought to equilibrium at the desired values, the spark advance was set at the minimum at which uniform detonation could be maintained, and the compression ratio was varied until incipient detonation was observed on the cathode-ray oscillograph. The spark advance was then increased by suitable increments and the compression ratio was successively readjusted to give the same intensity of detonation. When an extreme spark advance was reached, detonation was no longer uniform. The engine speed was then changed and the procedure repeated.

Three series of runs were made at engine speeds of 800, 1600, and 2400 rpm and at a constant inlet-mixture temperature of 120° F. The different engine speeds were used to study the effect of speed on detonation at constant volumetric efficiency. Data taken for these runs are given in table I\* and are plotted in figure 7. The data are plotted merely to show that the points fall neatly on smooth curves, indicating good experimental control. Points at the right-hand ends of the curves, corresponding to abnormal spark advances, do not represent true maximum permissible pressures (although they may represent true maximum permissible compression ratios), because in these particular runs detonation occurred before peak pressure. In the discussion that follows, the maximum permissible pressure for these runs is taken as the pressure at which detonation actually occurred.

Pressure crank-angle indicator diagrams taken for the runs are reproduced (half size) in figures 4, 5, and 6.

About half an hour was allowed after each change of compression ratio to establish equilibrium and to make small adjustments to fuel and air quantities.

It was intended originally to make the runs with commercial iso-octane because of its homogeneity and also by way of comparison with results in reference 9. It was very difficult, however, to make the engine detonate satisfactorily at 2400 rpm with this fuel, and the only alternative was to use a fuel of lower octane

---

\*Runs were also made at inlet-mixture temperatures of 160° and 200° F, but these runs are not discussed because there was not sufficient time available to make a complete analysis. The experimental data for these runs, however, are included in table I. The authors intend to analyze these data at a later time.



rating. The runs were therefore made with standard reference fuel C-12, rated at 78.9 octane by the CFR motor method. Cyclic reproducibility with this fuel was not so good as that obtained with iso-octane.

The pressure of the unburned charge was determined by taking a pressure-crank-angle indicator diagram for each run with the M.I.T. balanced pressure indicator. The instant at which detonation occurred was determined by taking a  $dp/dt$  record for each run, but these  $dp/dt$  records are not shown in this report. When the films were developed at the completion of the test, it was found that the line of zero rate of change was badly distorted by spark pickup originating in the amplifier used with the photographic oscillograph. The time scale was not distorted, however, and the instant (or crank position) at which detonation occurred was clearly and accurately defined in most cases. When the records showed detonation to have occurred at some instant before peak pressure, the pressure at this instant as determined from the indicator diagrams was taken as the true maximum permissible pressure.

#### DISCUSSION OF EXPERIMENTAL RESULTS

In order to discuss the experimental results clearly, it is necessary to define delay precisely. The usual concept of delay is associated with the experiments of Tizard and Pye (reference 6). It was in these experiments that ignition lag or delay was first recognized. Tizard and Pye compressed a combustible mixture in a cylinder and recorded the pressure changes with time. They found that, if the mixture was compressed rapidly to, or above, a certain temperature called its "ignition temperature," there would be no explosion until after a definite time had elapsed.

This process can be represented by the curve of figure 8. Here a rapid adiabatic compression is carried out from O to A. At A, compression is discontinued and the pressure is maintained constant. If the temperature at A is above the ignition temperature of the gas, then an explosion will occur later at B. The interval AB has been referred to as the delay period. In this report it will be referred to as the "apparent delay." Apparent delay will be defined as the time interval between the end of isentropic compression and the instant of explosion. If the temperature at A is slightly below the ignition temperature of the gas, no explosion will result regardless of how long the



pressure and the temperature are maintained at this level; that is, for practical purposes, the gas will have infinite delay.

In the case of isentropic compression, the process can be completely specified by giving the initial conditions and the pressure-time history or the temperature-time history of the gas. In the following paragraphs, it will be assumed that the initial conditions are the same and that the compression is isentropic; thus, only the pressure-time history will be used. It will also be assumed that the combustible mixture consists of petroleum vapors and air.

Although the experimental demonstration and measurement of delay as effected by Tizard and Pye (reference 6) is straightforward enough, difficulty is encountered when the concept is used to clarify the mechanism of engine detonation.

A significant feature about the compression of the end gas in a detonating engine is that the compression is continuous up to the instant of detonation. Under these circumstances the concept of apparent delay is inconvenient. In figure 9, if the gas is compressed along  $OA_1$  to  $P_1$ , the minimum ignition pressure, the resulting apparent delay will be  $t_1$ . If the gas is compressed continuously from 0 to  $P_2$  along  $OA_2$ , the apparent delay period will be shortened to  $t_2$  (reference 13) and, if the gas is compressed continuously from 0 along  $OA_3$ , a pressure  $P_3$  will be ultimately reached, at which the apparent delay will be zero.

In a detonating engine, the unburned part of the charge is compressed continuously until spontaneous ignition results, and therefore the apparent delay period must always be zero. In order to avoid this difficulty, delay might be defined as the time interval between the instant at which the minimum self-ignition pressure is reached and the instant of explosion. With compression only to  $P_1$  (fig. 9) this definition gives the same value of delay as the preceding one, but, when continued to pressure  $P_3$ , along the same path of compression, the second definition gives the delay as  $t_3$ . It will be convenient to refer to delay defined in this manner as "total delay."

As a result of the use of this definition, it follows that, if a combustible mixture is compressed continuously along different paths which do not cross above the lowest ignition



pressure, then the path that has the smallest total delay will have the greatest self-ignition pressure. This fact is evident from a consideration of figure 10 where the total delay associated with the path OAC must be less than that associated with the path OAB since pressure and temperature are higher at any instant along AC.

The principle just illustrated is borne out by the engine experiments. The compression lines of the pressure-crank-angle diagrams of figures 4, 5, and 6 are shown plotted on a pressure-time basis in figure 11. These curves represent the pressure-time history of the unburned charge, which in most cases detonated at the point of peak pressure. The apparent delay is zero in every case, but the total delay can be determined if the minimum self-ignition pressure is known.

If 150 pounds per square inch is assumed to be the minimum self-ignition pressure and if all paths are shifted in time so that they start from a common point A on the line  $P_1 = 150$ , then it will be seen that the principle stated is borne out. If 150 pounds per square inch gage is, indeed, the minimum self-ignition pressure, it is allowable to shift these curves in time because the part of the paths below the minimum ignition pressure is of no significance as far as the ultimate self-ignition is concerned. A justification of this artifice based on the theory of chain reactions will be found in appendix D.

It will be noticed in figure 11 that, whenever two paths do not cross, the path that lies above the other at every instant has the highest permissible pressure and the smallest total delay. Paths 6, 7, and 34 have been corrected to allow for the fact that detonation did not occur at peak pressure. The pressure at which detonation occurred for these runs is indicated by crosses on the diagrams. When the paths cross, no conclusions can be drawn except that the results of such crossings do not contradict the principle. Small discrepancies may be accounted for by the fact that the temperature of the unburned charge at A varied slightly for the various runs.

In most of the runs spark ignition occurs before point A is reached, which complicates the computation of the temperature of the unburned charge at this point. A much more accurate temperature estimate can be made at some point prior to spark ignition because then the formula  $PV = BT$



where

P     pressure  
 V     volume  
 B     gas constant  
 T     temperature

can be used and good pressure and volume measurements can be obtained. (See appendix A.) A point at  $P = 50$  pounds per square inch absolute was selected, and the temperatures here for all the runs of figure 11 were computed. These temperatures were found to be constant within  $\pm 3$  percent. It is believed that the precision of these computations is better than  $\pm 2$  percent. (See appendix A.) The 3-percent variation at this point thus appears to represent a real, though small, temperature variation. The compression process being considered isentropic, it follows that the temperature variation of the unburned charge at A, where  $P = 150$  pounds per square inch gage will have the same variation. Thus, granted a small temperature variation at A, two identical compression paths would give slightly different maximum permissible pressures.

If the minimum ignition pressure is selected at  $P_1 = 125$  pounds per square inch gage, contradictions are encountered that are too glaring to be included in the range of experimental errors or slight temperature variations at  $P_1$ . The most significant of these contradictions is evident in the case of runs 1 and 27. The compression lines for these two diagrams are shown in figure 11 at  $A_1$ . It will be noticed that, although pressures are always higher at any instant along the curve for run 27, the peak pressure is the same as the peak pressure for run 1. This result contradicts the foregoing theory. This contradiction and other contradictions exist when A is taken at any pressure below 150.

When A is selected at a pressure greater than 150, say  $P_1 = 175$  pounds per square inch gage, a result like that shown at  $A_2$  is obtained. Again, only the compression lines for runs 1 and 27 are shown, and it will be observed that pressures are now higher at any instant along run 1, although the peak pressures are equal. This result also contradicts the theory. When the minimum ignition pressure is taken at  $P_1 = 150$ , as



at A, however, it will be noticed that the paths of runs 27 and 1 cross and therefore the equality of maximum permissible pressure can be justified. A careful study of these contradictions and inconsistencies showed that the observed facts fitted the theoretical reasoning best when the minimum ignition pressure was taken at  $P_1 = 150$  pounds per square inch gage. It may thus be concluded that, with a given composition and initial pressure and temperature, if the rate of compression of the unburned charge is increased, the maximum permissible pressure is higher.

#### SUGGESTIONS FOR FURTHER STUDY

It is suggested that a new experimental method of attacking the detonation problem be investigated. This method is suggested by the  $dp/dt$  record of figure 12. Here the pressure disturbances set up in the cylinder under conditions of moderate detonation are clearly shown. The instant at which detonation occurs is precisely defined, and the corresponding piston position and cylinder volume can be readily determined. A pressure-time record, taken simultaneously with the  $dp/dt$  record, would give the cylinder pressure at any instant. From these data the temperature and pressure of the end gas could be computed by the method used in the present investigation, and the pressure-time history would be recorded. The quantity of end gas igniting spontaneously or, in other words, the intensity of detonation would be immaterial.

This method has particular advantages over the maximum-permissible-pressure or critical-compression-ratio methods. By use of this method it would be possible to study the effect of changing a single engine variable such as spark advance. Such a change would not necessitate a change in compression ratio. The effect on detonation of products of combustion from detonating and nondetonating cycles could also be conveniently studied. This study might be made by running the engine under conditions of no detonation, then causing the spark to be suddenly advanced (that is, during the time required for the exhaust, suction, and power strokes), and a record taken of the first detonating cycle, which would be a record of detonation as influenced by the products of normal combustion. The engine could then be run for a few cycles with the spark advance set at the preceding instantaneous value and a record could be taken of the last cycle, which would be a record of detonation as influenced by the products of detonating combustion. The effect of contributions from the residual gases on pressure-temperature-time effects could then be readily determined.



The method presents other advantages. Detonation could be made to occur before peak pressure, which would shorten the crank angle interval between the occurrence of spark and detonation. A reduction would thus be made in the number of errors introduced in end-gas temperature computations due to the assumption that compression of the end gas is isentropic. (See appendix A.) It would also allow much easier control over the weight of charge per cycle because of constant clearance volume and would render unnecessary the use of an engine having a variable compression ratio.

This method might have a disadvantage in that different degrees of detonation would alter average combustion-chamber temperatures, but these temperature changes would not be objectionable where only a single detonation cycle is studied and should be of small account where only five or six detonating cycles are studied.

It is suggested that the fuels mentioned by Barnard (reference 14 and appendix E) be tested by this new method.

#### CONCLUSIONS

The results of this investigation show that:

1. Higher maximum permissible pressures can be used if the rate of compression of the end gas is increased.
2. Experimental data in engine detonation should be accompanied by the pressure-temperature-time history of the unburned charge in order that fundamental conclusions may be drawn.

Massachusetts Institute of Technology,  
Cambridge, Mass.



## APPENDIX A

## TEMPERATURE COMPUTATIONS

## FORMULAS AND CONSTANTS USED IN P-V-T RELATIONS

## FOR THE UNBURNED CHARGE

## Notation Used

The value of pressure  $P$ , specific volume  $V$ , and temperature  $T$  for the unburned charge at the point  $O$  is given the subscript  $o$ . The value of  $P$ ,  $V$ , or  $T$  for the unburned charge at any point between  $O$  and peak pressure is given the subscript  $x$ . The additional subscripts 1, 2, 3 on the  $x$  designate different computed values of the same quantity, thus:

$T_{x_1}$  indicated temperature of the unburned charge, that is, temperature computed from relation  $PV = BT$ , where  $P$  is measured on indicator diagram and  $V$  is determined from crank angle and weight of charge. These temperatures are considered nearest to true values.

$T_{x_2}$  adiabatic temperature of unburned charge computed from ratio of initial and final cylinder pressures, which are measured from indicator diagram.

$T_{x_3}$  adiabatic temperature of unburned charge computed from ratio of initial and final cylinder volumes, which are determined from crank position.

This system avoids confusion with the usual notation of  $T_1, T_2, T_3$ , etc. used to represent temperature at various points in the cycle.

In the following formulas other symbols used may be defined as follows:

$B$  gas constant

$c_v$  specific heat at constant volume, Btu/lb/°F



$c_p$  specific heat at constant pressure, Btu/lb/°F

### Formulas

$$PV = BT \quad (1)$$

Gasoline-air mixture containing about 5 percent burned residual gas, fuel-air ratio = 0.078.-

$$B = 50.8$$

$$c_p = 0.214 + 6.16 \times 10^{-5} T$$

$$c_v = 0.149 + 6.16 \times 10^{-5} T$$

(There is a slight error in the printed values of  $c_p$  and  $c_v$  of table VII, reference 9. The values given here are the correct ones.)

$$\log T_{x_2} = \log T_o + 0.304 \log \frac{P_x}{P_o} - 0.000125 (T_{x_2} - T_o) \quad (2)$$

$$\log T_{x_3} = \log T_o + 0.438 \log \frac{V_o}{V_x} - 0.000179 (T_{x_3} - T_o) \quad (3)$$

Gasoline-air mixture, no burned residual gas, fuel-air ratio = 0.079.-

$$B = 50.5$$

$$c_p = 0.211 + 3.19 \times 10^{-5} T$$

$$c_v = 0.147 + 3.19 \times 10^{-5} T$$

$$\log T_{x_2} = \log T_o + 0.307 \log \frac{P_x}{P_o} - 0.0000656 (T_{x_2} - T_o) \quad (4)$$

$$\log T_{x_3} = \log T_o + 0.443 \log \frac{V_o}{V_x} - 0.0000947 (T_{x_3} - T_o) \quad (5)$$

Air only.-

$$B = 53.34$$

$$c_p = 0.220 + 3.06 \times 10^{-5} T$$



$$c_v = 0.1515 + 3.06 \times 10^{-5} T$$

$$\log T_{x_2} = \log T_o + 0.311 \log \frac{P_x}{P_o} - 0.0000603 (T_{x_2} - T_o) \quad (6)$$

$$\log T_{x_3} = \log T_o + 0.452 \log \frac{V_o}{V_x} - 0.0000878 (T_{x_3} - T_o) \quad (7)$$

#### Remarks

1. Temperatures are in °F absolute
2. Specific-heat equations hold only for the range from 720° to 1900° F absolute
3. Logarithms are to the base 10
4. The values of  $T_{x_2}$  and  $T_{x_3}$  are determined from the transcendental equations by trial
5. Weight of burned residual gas is computed from thermodynamic charts
6. Weight of unburned residual gas (for nonfiring runs) is computed on the assumption that the residual gas is at exhaust-tank pressure and inlet temperature at the beginning of the suction stroke
7. The derivation of the true adiabatic equation for variable specific heats will be found in reference 15 and information on the specific heats will be found in appendix C of reference 9

#### COMPUTATION OF END-GAS TEMPERATURE

Although this investigation was concerned mostly with the relation between the rate of compression of the end gas and its maximum permissible pressure, it was of interest to calculate the resulting changes in end-gas temperature and relative density.

The method of calculating end-gas temperature was, in general, the same as that given in appendix B of reference 9; that is, the pressure and the specific volume of the unburned charge were



measured at some point on the compression line of the indicator diagram and from these values the temperature of the charge was computed. The temperature rise of the end gas, caused by compression by the piston and the expanding gases behind the flame front, was computed by assuming isentropic compression. The contribution of residual gas and the variation of specific heat with temperature were allowed for exactly as in reference 9.

The slight differences in the two methods are outlined as follows:

In reference 9, interpolation was necessary to determine appropriate values of air consumption and maximum permissible pressure; whereas in the present work these values were measured directly and no interpolation was required.

In reference 9 the point on the compression line chosen for the base of end-gas temperature computations was 146° B.T.C. It was found in the present work that inaccuracy was introduced by assuming isentropic compression from a point so early in the cycle (see section on Precision in this appendix) and the base of computations was therefore moved as near top center as possible. The limit on this procedure is spark advance, for after ignition the specific volume of the unburned charge can no longer be determined from indicator diagrams.

Instead of using a definite crank angle for the base of end-gas computations, however, a definite pressure, 50 pounds per square inch absolute, was first selected and the corresponding crank angle determined from the indicator card. The specific volume of the cylinder contents at this point was then computed, and the temperature at this point was determined from the gas equation  $PV = BT$ . This procedure provides a more convenient basis of comparison. Cylinder pressures reach 50 pounds per square inch absolute before spark ignition in every run.

The principal data used in end-gas computations are given in table II. The computations for the weight of residual gas have been omitted, as this procedure is identical with that used in reference 9. Equations 1 and 2 were used in making maximum end-gas temperature computations. Maximum relative end-gas density was determined by dividing maximum end-gas pressure by maximum end-gas temperature.



## PRECISION OF TEMPERATURE COMPUTATIONS

The problem of determining the temperature of the unburned part of the charge may be stated briefly as follows:

Given the pressure, volume, and weight of charge at some point O on the compression line of the indicator diagram, to determine the temperature  $T_x$  of the unburned part at any point x between O and peak pressure. (The point O should not be confused with the point A mentioned in the discussion. The point O is arbitrarily selected as a base of computations; whereas the point A has a definite location determined by the state of the charge.)

### Principal Factors Causing Errors in Temperature Computations

The principal factors that introduce errors into the computed value of  $T_x$  are:

1. Accuracy of the method used to compute  $T_x$  from the conditions at point O
2. Reliability of the adiabatic assumption
3. Accuracy of determining the conditions at point O
4. Location of point O
5. Accuracy of air measurements
6. Accuracy of clearance volume measurements

These factors, as well as some miscellaneous factors, are investigated herein:

### Methods used to compute $T_x$ . - Three methods can be used to

calculate the temperature of the unburned charge. The first method involves the relation  $PV = BT$  where P is measured on the indicator diagram; V is determined from the weight of charge and cylinder volume (specific volume); and B, the gas constant, is determined by the method given in appendix C of reference 9. Temperatures so determined are here called indicated temperatures and are considered to be closest to the



actual values; they are designated  $T_{x_1}$ . This method is of no use after the passage of spark unless the specific volume of the unburned charge can be determined. In this work the specific volume of the unburned charge after the passage of spark was unknown.

The second method involves one of the true adiabatic equations (2), (4), or (6) already given in this appendix (the particular equation depends on the charge composition), where temperature is expressed as a function of cylinder pressure as measured on the indicator diagram. Temperatures so determined are designated  $T_{x_2}$ . Since this method is independent of volume, it can be used after the passage of spark.

The third method involves one of the true adiabatic equations (3), (5), or (7) (the particular equation depends on charge composition), where temperature is expressed as a function of the volume of the unburned charge. This method is independent of the indicator diagram except for the determination of the temperature at the point O. It cannot be used after the passage of spark. Temperatures so determined are designated  $T_{x_3}$ .

These three methods should give the same result for any point on the compression path where they can be applied, if the compression process is isentropic; but, under certain circumstances, there is considerable disagreement. This discussion is mostly an attempt to explain why these differences exist and to show how the methods can be brought into closer agreement.

Reliability of the adiabatic assumption.- A comparison of the three methods is made for run 27. Point O ( $P_O, V_O, T_O$ ) was taken at 100° B.T.C., and a light-spring indicator diagram was available; therefore, good measurements of pressure could be made at this point. The data are given in table III. The terms  $T_{x_1}$  and  $T_{x_2}$  cannot be computed after 5° B.T.C., because here the charge begins to burn. The agreement among the three temperatures is very good up to this point. Pressures and temperatures are plotted in figure 13. A reproduction of the actual indicator diagram is shown in figure 5.

These results show that the assumption of reversible adiabatic compression is sufficiently good up to the beginning of



combustion, where it may be checked. Unfortunately, further investigation gives conflicting evidence on this point.

Run 73, a nonfiring run, was made in order that temperatures computed by the three methods could be compared throughout the entire compression period. First, a check was made to see how closely firing and nonfiring records coincided on the compression stroke. The engine was thoroughly warmed up, after which an indicator card was taken with a 50-pound spring. The ignition switch was then cut and a motoring diagram was taken immediately on the same card. This composite card is shown in figure 14. It will be seen that conditions on the compression stroke are very nearly the same in both cases up to the point of ignition, 22° B.T.C. The motoring charge consisted of dry air and fuel.

Indicated and adiabatic temperatures computed from 100° B.T.C. for the nonfiring diagram are given in table IV. The plotted values appear in figure 15. There is a difference of 73° F between indicated and adiabatic temperature  $T_{x_3}$  at the peak, which would indicate that heat was being lost by the charge. The P-V diagram for this run, however, showed practically no difference between rising and falling pressures. This fact indicates that the process is reversible, and therefore the observed differences cannot be due to heat transfer or leakage.

This contradiction could be explained if the indicator recording mechanism were introducing a systematic error that was making the rising pressures appear lower and the falling pressures appear higher than the true values, thus obscuring the effects of heat transfer. A run, to be described presently, was made to check this theory.

The P-V diagram for run 73 plotted on log paper gave the value of the adiabatic exponent as 1.32.

Accuracy of determining the conditions at point 0.— The accuracy of the measurement of pressure at point 0 depends upon the accuracy of the indicator and the precision of the measurements of the indicator diagrams. The diagrams can be measured to  $\pm 0.01$  inch when the line is thin and regular and the slope not too steep. But even under these favorable conditions, the percentage error in reading the heavy-spring diagrams in the first half of the compression stroke may be considerable. In



the case of run 27 (table III), if the pressure is measured at 100° B.T.C. on the heavy-spring diagram (150-lb spring), an error of 0.01 inch results in an error of 1.5 pounds per square inch. This error is sufficient to change the indicated temperature at this point from 873° F absolute to 941° F absolute and the peak temperature  $T_{x_2}$  from 1705° F absolute to 1790° F absolute.

It has been found in this laboratory (reference 16) that the accuracy of diaphragm units is poor when small pressures are being measured, owing to the force required to overcome the elasticity in the diaphragm which varies somewhat with different conditions of operation. This error has a maximum value of 2 pounds per square inch. An error of this magnitude at 100° B.T.C., in the case of run 73, is more than sufficient to account for the differences in maximum temperatures. Thus, if the true pressure at 100° B.T.C. were 2 pounds per square inch lower than that given in table IV, the true maximum indicated temperature would be diminished to 1175° F absolute and the maximum adiabatic temperature  $T_{x_3}$  would be diminished to 1145° F absolute. Under these circumstances the adiabatic temperature is 30° F lower than the indicated temperature. This difference would indicate that heat was gained in the compression process.

The diaphragm error can be eliminated by the use of a flapper-valve type of cylinder unit; but, if light-spring diagrams were taken with the flapper-valve unit in addition to the heavy-spring diagrams for runs 1 to 59, the required amount of testing time would have been approximately doubled and the undesirable situation of using the data from two separate runs for computing a single result would have resulted because of the necessity of shutting down the engine to change units. A few light-spring diagrams were taken, however, either before the beginning of a given series of runs or at the conclusion.

Although a diaphragm error of 2 pounds per square inch in the early part of the compression stroke would be sufficient to explain the temperature differences, it is not certain that the maximum value of this error was always in evidence. Accordingly, the theory that the indicator recording mechanism was introducing a systematic error which made the rising pressures appear lower and the falling pressures appear higher than the true values was considered. An error of this nature would be introduced if the viscosity of the oil in the indicator plunger were great and if the compression side of the card were taken while the indicator pointer was moving outward and the expansion side taken while the pointer was moving inward.



This effect was investigated by means of a nonfiring run, run 76. The engine was warmed up, the ignition cut, and a motoring card taken. The following precautions were observed in using the indicator: The cylinder and the plunger were thoroughly cleaned and a very light oil was placed in the reservoir to diminish viscosity effects. The pointer was pumped up to near the end of its stroke and then allowed to descend very slowly with the pump turned off and the contactor switch on "make." This procedure gave the compression side of the diagram. The contactor switch was then turned off and the pointer again pumped up to near the end of its stroke and allowed to descend slowly, at approximately the same speed as before, with the contactor switch on "break." This procedure gave the expansion side of the diagram. Asymmetry of the diagram, which might be introduced by friction and viscosity in the indicator mechanism, was thus greatly reduced. The diagram is shown in figure 16. There was considerable improvement in detail that does not show to advantage in the reproduction.

Peak temperatures for run 76 were computed from  $100^{\circ}$  B.T.C. The results are given in table V and the curves in figure 17. Maximum  $T_{x_3}$  is  $171^{\circ}$  F higher than maximum  $T_{x_1}$ .

If values of  $T_{x_3}$  are substituted in equation (1), the values of corresponding cylinder pressures  $P_{x_3}$  are obtained: that is, the pressures which should exist if the process were adiabatic. These values are given in the last column of table V. The maximum difference is 21 pounds per square inch at the peak.

In view of the precautions taken with this run, it is clear that the discrepancies are certainly not due to the supposed systematic errors of the indicator. The disagreement can be explained if the maximum error of the diaphragm unit is assumed to operate in conjunction with an error of 0.016 inch on the low side in reading the indicator diagram to give a pressure 2.8 pounds per square inch lower than the true value of  $100^{\circ}$  B.T.C.

If this run is compared with the preceding one, run 73, it will be observed that there is  $108^{\circ}$  F difference in the maximum values of  $T_{x_3}$ . Fuel and air consumption, compression ratio, speed, and so forth, were the same in both runs, but the inlet temperature was  $6^{\circ}$  higher in run 76 than in run 73. This condition does not account for the difference, because runs made at different inlet temperatures (to be described later) show no variation of this magnitude.



The pressure at 100° B.T.C. should be the same for the two runs, but it will be observed (tables IV and V) that  $P_0$  is 18.6 pounds per square inch for run 73 and 20.3 pounds per square inch for run 76. An error in measuring the indicator diagram of  $\pm 0.01$  inch would account for  $\pm 0.5$  pound per square inch difference, and the remainder may be accounted for by the diaphragm error. Since the runs were made under practically identical conditions, the temperatures at 100° B.T.C. are proportional to the pressures at that point (from  $PV = BT$ ). The temperature at 100° B.T.C. for run 73 is 717° F absolute and for run 76 is 785° F absolute. This initial temperature difference is responsible for the large difference in maximum values of  $T_{x_3}$  for the two runs.

Location of point O.—Adiabatic temperature computations so far considered in this appendix were based on cylinder conditions at 100° B.T.C. It is desirable to see what effect the location of this point has on maximum adiabatic temperatures.

Three indicator cards, numbers 5, 37, and 51 from the work of reference 9, were examined for this effect. The cards were for runs at approximately the same fuel-air ratio but with inlet-mixture temperatures of 200° F, 120° F, and 80° F, respectively. The maximum end-gas temperature for each run was computed from 146°, 100°, and 30° B.T.C. by the use of equation (2). The results are given in tables VI, VII, and VIII.

The maximum end-gas temperatures should be the same in any one of these runs, regardless of the location of the point O, inasmuch as only one method of computation was used. This agreement is very good in the case of run 37 and is within 1 percent in the case of run 51. There is a 1.3-percent variation in the case of run 5, which is of the same order as the experimental precision and therefore satisfactory. It is worth noticing, however, that light-spring indicator diagrams were available for these runs.

The effect of the location of the point O on the three methods of temperature computation was studied for the case of run 76. A 50-pound spring was used in taking the indicator diagram for this run. The point O was selected at 40° B.T.C. and temperatures were computed by means of equations 1, 4, and 5. The results are given in table V and the curves are plotted in figure 18.



Notice that the maximum difference in temperature is now only 48° F and the difference between adiabatic and indicated pressures is now less than 6 pounds per square inch. Although these differences are much less than when the maximum values were computed from 100° B.T.C. (see table V), yet the absolute correction necessary to apply to the pressure at 40° B.T.C. in order to eliminate the 40° F difference is about the same (2.65 lb/sq in.) as was necessary to eliminate the 171° F difference when the maximum values were computed from 100° B.T.C. This fact points strongly to the presence of a zero error in the diaphragm.

It was shown that an error of 0.01 inch in measuring pressure on the heavy-spring diagram at 100° B.T.C. for the case of run 27 resulted in a variation in maximum  $T_{x_2}$  of 85° F. If this same error were made at 40° B.T.C., the variation in maximum  $T_{x_2}$  would be only 10° F.

From the foregoing considerations it is apparent that, when heavy-spring diagrams only are available, it is desirable to locate the point 0 early on the line of rising pressures, where the slope is gentle, in order to facilitate measurement; but a compromise must be made between this location of the point and a location later in the cycle, which would be desirable for reducing the percentage of diaphragm errors. Moreover, the nearer the point 0 is to the point x, the less error will be involved in calculating the temperature at point x from that at point 0. A good compromise location for runs 1 to 59 was between 40° and 50° B.T.C.

Accuracy of air measurements.- In the case of nonfiring runs it might be expected that the air consumption per cycle would increase with time after cutting the ignition due to the cooling of the cylinder walls. Since the compression side of the indicator diagram was taken first, it might be expected that less air would be drawn into the cylinder during this period than during the period required to take the expansion side of the diagrams. This variation would be averaged over the complete cycle by the method used in making air measurements.

In order to detect this change, if any, three indicator diagrams - runs 77a, 77b, and 77c - were taken in succession. The engine was warmed up for about 30 minutes, the ignition and the fuel were shut off, and dry air only was admitted to



the engine. An air measurement was taken for each card. The last card was finished 8 minutes after cutting the ignition. No significant change in air consumption was observed. The air-meter readings for the three runs were 58.8, 59.0, and 58.9 rpm, respectively; and the peak pressures were 147.5, 148.5, and 147.0 pounds per square inch, respectively. This variation is less than 1/5 percent. The inlet temperature varied from 126° F to 128° F during the runs, which is also a negligible variation. Speed was kept constant with a strobotac; hence there should be no asymmetry introduced in the motoring card due to cylinder cooling. It is possible, of course, that all the cooling took place in the brief interval between the time ignition was cut and the beginning of the first card, but, again, asymmetry should not be introduced.

Temperature-pressure data for run 77a appear in table IX and are plotted in figure 19. Maximum  $T_{x_3}$  is 75° F higher than the maximum indicated temperature. If the pressure at 100° B.T.C. were reduced by 1.2 pounds per square inch, these two maximum temperatures would be equal. This result is well within the maximum error of the diaphragm. The P-V diagram for this run showed a very small difference between the compression and expansion lines, the expansion line being slightly lower.

A further question to be settled was the effect of absolute errors of air measurements on temperature computations. Various values of air consumption per cycle were assumed, and corresponding maximum adiabatic temperatures and indicated temperatures were computed from 100° B.T.C. for run 77a. The results are shown in figure 20. The actual measured weight of total air charge per cycle for run 77a was 0.00125 pound, which includes the residual air in the clearance space, and assumed values ranged from 0.0008 to 0.0013 pound per cycle. It will be seen from the curves that a large error in air measurement has a relatively small effect on the difference between maximum  $T_{x_3}$  and  $T_{x_1}$ , since the curves run nearly parallel. The variation in indicated temperature at 100° B.T.C. is also shown.

Accuracy of clearance-volume measurements.- The observed fact that the adiabatic temperature computed from the pressure ratio is lower than that computed from the volume ratio could be readily explained if the clearance volumes were in error. At the beginning of this work, the compression ratio micrometer



was so set that, at zero reading, it corresponded to a compression ratio of 10.00 with a clearance volume of 68 cubic centimeters. The clearance volume was measured by pouring oil into the cylinder from a graduate with the piston at top center. This measurement was made with the various spark-plug holes fitted with blind plugs.

When the temperatures were computed and the large discrepancies were observed, another check was made and showed the clearance to be somewhat larger. An effort then was made to determine the clearance more accurately.

Dependence on graduates was avoided by determining the weight of water necessary to fill the clearance volume. Great care was taken to eliminate any entrapped air bubbles. These measurements could be repeated to a precision of 0.3 percent, which was never the case when graduates and oil were used. There was very little leakage of water past the piston. The fall in the level of the water in the vertical spark-plug hole was observed to change about 0.1 cubic centimeter after a minute or so. It took only about 15 seconds to fill the clearance space; hence there could be no appreciable error from this source. The water in the clearance space was blown out with compressed air, and the engine was fired for a few minutes after making the measurement.

The same spark-plug,  $dp/dt$  unit, and balanced pressure unit used in the runs were in the cylinder head when these measurements were made. A change in spark plugs of different types may cause a change in clearance volume of 0.5 cubic centimeters. This figure is significant in careful work at high compression ratios.

A glance at figure 21 shows how errors made in measuring clearance volumes affect maximum values of  $T_{x_3}$  and  $T_{x_1}$ . These curves were computed for the conditions of run 77a. An increase in measured clearance causes an increase in maximum indicated temperature and a decrease in maximum adiabatic temperature  $T_{x_3}$ . The intersection of the two lines shows the value the clearance volume should have in order to make the two temperatures equal. This occurs at 77.6 cubic centimeters; whereas careful measurement of the actual clearance volume for this run gave 72.5 cubic centimeters. Although an error of this magnitude would readily explain the fact that  $T_{x_3}$  is consistently higher than  $T_{x_1}$  in all the runs considered, it is quite certain that no such error from this source existed.



The variation of indicated temperature at 100° B.T.C. was 772° ±2° F absolute for the range of clearance-volume errors considered. It is not known how much change occurs in clearance volume with temperature. The change probably is negligibly small because the linear expansion of the piston and the connecting rod would be offset somewhat by the linear expansion of the cylinder. Assumption that only the cylinder expanded gave insufficient change in volume to account for the observed effect.

The clearance volume should change somewhat when the engine is running because of the deflection of the connecting rod, crank, cylinder walls, and so forth, under gas pressure. This effect would be offset somewhat by inertia forces in the piston and connecting rod near top center on the compression stroke. An estimate of this effect was made by pumping oil under pressure into the combustion chamber with the piston at top center. A dial gage was adapted to a pin fitted through a blind plug screwed into the vertical spark-plug hole in the top of the cylinder. The pin was made to press firmly against the piston by means of a spring. Any motion of the dial gage gave the relative displacement between the piston and the cylinder head. It was found that the relative displacement was 0.001 inch per 100 pounds per square inch pressure up to the maximum pressure used, which was 1000 pounds per square inch. For the case of run 77a this displacement would result in a difference between measured and actual clearance volumes at top center of about 0.2 percent, which is small enough to neglect.

#### Miscellaneous Factors Causing Errors in

##### Temperature Computations

In order to eliminate the effects of any unforeseen engine idiosyncrasies, the high-speed CFR engine was replaced by a low-speed CFR engine. The clearance volume of the low-speed engine was carefully measured as described. Runs were made with this engine at two different engine speeds and inlet temperatures. The same indicator and diaphragm units were used.

The first run, run 78, was a nonfiring air run made under approximately the same conditions as run 77a. The air was not dried and was measured with an orifice instead of an air meter. The data for run 78 are presented in table X and figure 22. Notice that pressures and temperatures are considerably lower in run 78 than in run 77a but that temperature differences are



about the same. The higher values of run 77a may be accounted for by the fact that inlet temperature and compression ratio are slightly higher. But comparisons are complicated by the fact that the inlet valve closes at  $140^{\circ}$  B.T.C. in the case of run 77a and at  $154^{\circ}$  B.T.C. in the case of run 78. Light-spring diagrams were not taken for these two runs so that the exact pressure at inlet-valve closing is unknown.

Another nonfiring run, run 79, was made on the low-speed engine under the same conditions as run 78 except that the speed was reduced to 800 rpm (see table XI and fig. 23). The air consumption was somewhat higher on this run. It is apparent that the differences in computed cylinder temperatures are almost the same, showing that engine speed does not affect the difference materially.

Finally another air run, run 80, was taken on the low-speed engine at 800 rpm with the inlet temperature increased to  $191^{\circ}$  F (see table XII and fig. 24). Although the temperatures are all higher, the differences are still apparent and considerably larger. Too rigid comparisons cannot be made because no attempt was made to keep the air consumption exactly the same in the three runs.

#### Effect of Charge Composition on Cylinder Pressure

The measured peak pressure  $P_{x_1}$  is 16 pounds per square inch higher in run 77a than in run 76, although operating conditions were the same. This difference can be accounted for by considering the number of mols for the two charges. The molecular weight for the fuel-air mixture is 30.6 and the molecular weight of air is 28.9. The total weight of fuel-air charge is 0.001285 pound or  $0.001285/30.6 = 0.0000420$  mol, and the total weight of air charge is 0.00124 pound or  $0.00124/28.9 = 0.0000429$  mol. At peak pressure the volume of charge is the same in either case. If the formula  $PV = NRT$  is applied, where

- V charge volume
- N number of mols
- R universal gas constant
- T temperature



there results for the air charge of run 77a

$$P_a V_a = 0.0000429 RT_a$$

and for the fuel-air charge of run 76

$$P_f V_f = 0.0000420 RT_f$$

Then

$$\frac{P_a}{P_f} = \frac{429T_a}{420T_f}$$

$$1.11 = 1.11$$

For any given cylinder temperature,  $P_a$  will therefore be higher than  $P_f$ .

#### A Fourth Method of Computing Adiabatic Temperature

An estimate of adiabatic cylinder temperature can be made by considering that all the temperature rise of the charge during compression is due to the work done by the piston and that no temperature rise is transferred to or from the cylinder walls. If the work done by the piston on the compression stroke is measured from the area of a P-V diagram, then the final temperature can be computed by solving for  $T_3$  in the equation

$$W = w \int_{T_0}^{T_3} c_v dT$$

where

W work done on charge by piston, ft-lb

w weight of charge, lb

$c_v$  specific heat of charge at constant volume, Btu/lb/°F

$T_0$  indicated temperature at 100° B.T.C., °F abs.



$T_3$  adiabatic temperature at top center, °F abs.

For the case of run 77a this equation becomes

$$0.016 = 0.00125 \int_{776}^{T_3} (0.1515 + 0.0000306T) dT$$

$$T_3 = 1340^\circ \text{ F abs.}$$

This value lies about midway between the peak values of  $T_{x_1}$  and  $T_{x_2}$ .

This method is considered not so accurate as the other methods used because it is always difficult to trace a P-V diagram and measure the area with any great precision. The method is included here merely as a rough check on values computed by the other methods.

### Conclusions

Large variations in speed, inlet temperature, and air consumption do not account for the difference between indicated (true) and computed adiabatic temperatures. Errors in measuring the indicator diagram may be a contributing cause in some cases, but the difference has a consistency that eliminates this source as a general explanation. Small errors in clearance volume measurement will alter the difference appreciably at high compression ratios. The elasticity of the diaphragm in the indicator unit is probably responsible for the major part of the discrepancy. Whenever the state of the end gas is investigated by the methods outlined in this report, light-spring flapper-valve indicator diagrams should be taken simultaneously with the heavy-spring diagrams.

It may be concluded that the end-gas temperatures for the detonation runs are, in general, about 25° F lower than the given adiabatic values. This fact should not affect the main conclusions arrived at in this report inasmuch as all temperatures should be affected alike. This estimated error would be subject to revision if the effect of heat transfer from the burned to the unburned part of the charge were considered. It might well be that this heat transfer, if any, is sufficient to make the actual temperatures approach more nearly the computed values.



## APPENDIX B

## DISCUSSION OF FLAME PHOTOGRAPHS IN

## REFERENCES 10, 11, AND 12

The photographic combustion studies of references 11 and 12 were taken at 40,000 exposures per second or at about 18 times the speed at which those of reference 3 were taken. The photographs of detonating combustion taken by Rothrock and his co-workers in references 10, 11, and 12 are in agreement with those of Withrow and Rassweiler in reference 3 to the extent that detonation appears to be a rapid reaction in the end zone but are at variance with those of Withrow and Rassweiler in that the reaction does not appear always to take place ahead of the flame front.

The general conclusion reached by the authors of references 10, 11, and 12 is that, although autoignition of the last part of the charge may occur coincident with knocking, the knock itself is something which the data indicate may occur only in a portion of the charge which has already become inflamed before the knock occurs. The authors of the present report, however, believe that the photographs of references 10, 11, and 12 may actually be a confirmation of the autoignition theory of engine detonation.

In figure 5 of reference 11 frame M-9 shows the flame front approaching the end wall with darkening of the end zone presumably due to preflame reactions. In the next frame, M-10, the darkening of the end zone is such that the flame front can be no longer distinguished. It is stated in the text of this reference that knock occurs in frame M-11. Again, in figure 8, frame N-11 shows unburned charge near the edge of an unobservable region of the combustion chamber. Knock occurs, according to the text, in the next frame N-12. Thus, in both series of photographs that show knock in reference 11, detonation may be taken to occur in the unburned charge and can therefore be interpreted in support of the autoignition theory. Cases in which four flame fronts come together in the center of the combustion chamber have shown the four fronts apparently merging before detonation takes place. The flame front appears to be similar to a silhouette or skyline of a range of irregular mountains where only the highest mountains show. Any valleys that may lie between the mountains cannot be



observed. A cross section of the flame front at any level will therefore be more indented and more irregular than the silhouette. A simple explanation for the observation that the flame fronts appear to cross each other, as noted in reference 10, is that burning on the peaks of one flame front is occurring in the valleys of the other. If this explanation is correct, the presence of intersecting flames indicates unobserved regions of unburned charge.

It is well known that when the flame approaches a wall or another flame coming from the opposite direction, the observed progress of the flame is greatly slowed. This phenomenon can be explained as follows. The photographs show the boundary of the unburned charge. The volume enclosed is being diminished by two processes:

1. Physical compression
2. Burning at the boundary

Evidently when the volume of the unburned charge is large, the contribution of physical compression is large, and vice versa. In addition, when the unburned charge becomes small, the rate of liberation of energy and hence the rate of pressure rise may also be small owing to the reduced area of the flame front. Preflame reactions in the unburned charge, furthermore, may be of importance in suppressing compression of this part. The last part of the charge to be traversed by the flame, therefore, appears to burn slowly, and it is not surprising to note that detonation occurs a considerable interval after the apparent merging of flame fronts.

The particular apparatus used in references 10, 11, and 12 employed fuel injection into fresh air containing no residual gas. It is a common observation that fuel injection does not result in a homogeneous charge even when injection is into hot residual gas. This fact is indicated by the different mixture strengths for the limits of a combustible mixture that are noted when cylinder injection is used in place of premixed fuel and air. It seems probable that, with injection into relatively cold air, the mixture will be even less homogeneous than in the case of an engine with cylinder injection. Withrow and Rassweiler (reference 3) attribute irregularity of the flame in their experiments to nonhomogeneity of charge, although their engine was fed premixed fuel and air in the normal manner.



In the light of the evidence, the authors are of the opinion that:

1. The apparent depth of the flame front in the pictures of references 10, 11, and 12 is due to the mixture being less homogeneous in the apparatus used than in the normal engine.
2. Detonation, which occurs in the pictures of reference 12 apparently in the region already traversed by the flame, is probably in unobserved valleys of the flame front that the flame has not yet reached.
3. Until more damaging evidence is available, the auto-ignition theory is still tenable and is the simplest interpretation of the observed facts.

#### APPENDIX C

##### DESCRIPTION OF FUEL SYSTEM

The fuel system used in these tests was designed to accomplish the following ends:

1. Eliminate vapor lock
2. Supply sufficient pressure to the inlet of the fuel injection pump to insure reliable operation at high speed
3. Reduce to a minimum errors due to change in pressure head at the pump inlet when fuel measurements were being made
4. Eliminate personal errors in determining fuel-air ratio and improve the precision of measurement
5. Avoid the necessity of correcting fuel measurements for changes in specific gravity due to changes in temperature
6. Make the procedure of determining fuel-air ratios as simple as possible



Vapor lock was eliminated by maintaining the pressure in the fuel system at 48 inches of mercury gage. The pressure was maintained constant by feeding water from the city water mains into the bottom of the fuel drum A (fig. 3) through the pressure regulator B. The regulator was permanently set to give approximately the desired value, and fine adjustments were made by controlling the rate of efflux of the water by means of the small valve C. After the pressure was once set, it maintained its value within 0.1 inch of mercury with little or no attention. The fuel drum was of sufficient strength to eliminate fire hazard due to leakage or rupture.

Inasmuch as every effort was made to keep the engine inlet air dry, it was desirable to know if this dryness would be nullified by water dissolved in the fuel. It is practically impossible to have a dry charge. Some water vapor is always added to the fresh charge from the residual gases, and it is convenient to use this value as a basis of comparison for the effects of outside additions of water.

For a fuel-air ratio of 0.07 and a 10-percent residual gas content, the weight of fuel is about 0.06 pound per pound of charge and the weight of residual water is 0.009 pound per pound of charge, giving a ratio of  $\frac{0.009}{0.06} = 0.15$  pound of water per pound of dry fuel supplied. Water dissolves in gasoline to the extent of about 0.00005 pound per pound of solution at room temperature (reference 17). The ratio of dissolved water to residual water is  $\frac{0.00005}{0.15}$  or 0.03 percent, which is negligibly small.

The surge tank D was placed in the system to smooth out pressure pulsations from the regulator valve and also to bring the free surface of the fuel up to the same level as that in the balance can E. The surge tank was made from a lucite cylinder about 6 inches in diameter and 1/4 inch thick with brass heads held together by through bolts passing outside the cylinder. The use of transparent material allowed observation of the fuel level. The same construction was used in the balance can E with the exception that the heads were made of aluminum.

A mercury manometer was tapped into the surge tank as shown. When it was desired to fill the balance can, the valves F and G were closed and the valve H was opened slightly. This



procedure reduced the pressure in the can and fuel flowed into it when the three-way valve J was turned to the correct position. An objection may be raised to this method of filling the balance can. Some of the lighter ends undoubtedly escape, but the loss should be much smaller than that of fuel systems which use a measuring burette continuously open to the atmosphere. It requires only a very slight reduction in pressure to cause the fuel to flow rapidly.

This objection can be overcome simply by allowing the fuel from the surge tank to seek its level in the balance can. This method is slower; it takes about 1 minute for 0.10 pound to flow in this fashion.

It is not known whether air pressure on the fuel increases the rate of polymerization of the fuel to any appreciable extent. As far as could be ascertained, this effect is not serious.

The line leading to valve J was connected to an air pump (an ordinary automobile tire pump) that was used to force air into the system for the purpose of maintaining a constant fuel level in the surge tank.

The pressure head of the fuel is practically the same regardless of whether fuel is being drawn from the balance can or directly from the fuel tank. There is a very slight change in pressure while fuel is being weighed, but this change amounts to only about one-half inch of gasoline in 48 inches of mercury.

Considerable difficulty was encountered in finding a three-way valve that would handle gasoline at the operating pressure without leaking. The difficulty was finally overcome by using a plug valve having a monel metal cone and neoprene port seats. The port drillings of this valve are shown in figure 3.

It was thought that the neoprene tube connections to the fuel can might make the balance too insensitive, but checks made against an analytical balance showed the sensitivity of the fuel balance to be better than 1 part in 2000. The balance was made of aluminum (except for the knife edges) to reduce the load and inertia effects and was suspended from overhead to insulate it from engine vibration. A set of weights calibrated to read from 0.01 to 0.2 pound was found suitable for CFR engine operation at all speeds and fuel-air ratios. The electrical contacts on the balance were made of silver and gave good service.



When fuel measurements were made, the can was filled sufficiently to keep the contacts open when the weight was on the pan, and the two-way switch K was placed in position 1. When the pan descended, the electric clock and air-meter counter were started by the relay. The weight was then removed from the pan and the switch was placed in position 2. The relay was not affected by this change. When the balance again descended, the clock and counter were automatically stopped and the fuel weight, time, and air-meter revolutions were precisely known.

The air-meter counter was constructed from an ordinary gas-meter counter and a magnetic clutch taken from an electric stop clock. The counter was mounted on the air meter in plain view of the operator and was driven directly from the air-meter shaft. The rotameter gave a good check on variations in flow rate during any given run.

#### APPENDIX D

##### DISCUSSION OF THE IGNITION DELAY

###### Method of Isolating the Ignition Delay

It has been tacitly assumed that the concept of delay provides the only satisfactory explanation of the experimental fact that an increase in compression rate raises the maximum permissible pressure. It is not necessarily obvious that such is the case, however, and hence the assumption must be definitely established.

Consider runs 1 to 7. (See fig. 4.) The operating factors that varied in these runs were essentially spark advance and compression ratio. Slight variations in inlet-mixture pressure and exhaust pressure can be ignored because they were made solely to keep the weight of charge per cycle constant. The remaining operating factors, such as mixture composition, piston speed, inlet-mixture temperature, and humidity were maintained constant and can also be ignored. The only factors that can account for the observed changes in end-gas conditions are therefore: heat transfer, flame speed, and ignition delay.



The observed results might be supposed to be due to the effect of heat transfer. Thus if, under the conditions of these runs, it were found that, when more heat was transmitted to the unburned charge, the charge detonated at a lower pressure and that this heat transfer varied consistently with rate of compression, then an explanation based on ignition delay would be difficult to establish. Similarly, if a consistent correlation could be established between flame speed and permissible peak pressure, this correlation might be given as an explanation of the observed facts without any necessity for assuming a delay. It might be concluded that the effect of delay was negligible. If it can be shown, however, that heat transfer tends to produce trends opposite to those observed, then it must be concluded that the observed trends would be more pronounced if the heat transfer were zero.

The temperature of the cylinder walls should not be greatly above the coolant temperature of  $672^{\circ}\text{F}$  absolute. The temperature of the exhaust valve can be estimated from measurements made by C. G. Williams (reference 18). These measurements show that, in very small engines, exhaust-valve temperatures of  $1200^{\circ}\text{F}$  absolute are probably not exceeded, but, in the majority of automobile engines, temperatures of about  $1300^{\circ}$  to  $1375^{\circ}\text{F}$  absolute are readily attained and  $1475^{\circ}\text{F}$  absolute can be reached at high speeds. If the low speed of operation is considered, the temperature of the exhaust valve in the CFR engine at 800 rpm may be estimated at not more than  $1280^{\circ}\text{F}$  absolute. The temperature of the piston is undoubtedly considerably lower.

Consider runs 1 and 6 and let it be assumed that all combustion-chamber surfaces are at an average uniform temperature of  $1280^{\circ}\text{F}$  absolute in both cases. This value is an unreasonably high average to assume, but it is taken because it is unfavorable to, and simplifies, the following argument. Indicator diagrams for these two runs are shown in figure 25. The paths of compression from  $120^{\circ}\text{B.T.C.}$  to point P, where the compression lines intersect, are approximately the same. Calculations show that the temperature of the unburned charge of run 1 at P is  $1270^{\circ}\text{F}$  absolute and  $1290^{\circ}\text{F}$  absolute for run 6; hence, they are both equal to  $1280^{\circ}\text{F}$  absolute within the limits of experimental precision. From this point to peak pressure, the unburned charge will be cooled by the combustion-chamber surfaces. At pressure  $P_3$  the unburned charge of run 6 will have experienced less cooling due to its shorter time of contact with the surfaces, and



therefore the charge should detonate at a lower pressure than that of run 1. The true maximum permissible pressure in run 6, however, is 108 pounds per square inch (28 percent) higher, and therefore heat transfer between the unburned charge and combustion-chamber surfaces does not account for the observed results. This pressure difference is even greater between runs 1 and 7, but run 7 is not used, because under conditions of this run it was difficult to obtain good cyclic reproducibility.

If the effect of transfer of heat, or radiant energy, from the burned to the unburned charge were predominant, an effect opposite to that observed would be produced. In the case of run 1, spark occurs at top center and measurement of the  $dp/dt$  records shows that detonation occurs at peak pressure. Hence it may be assumed that a flame exists from spark to peak pressure; this interval occupies  $32^\circ$  of crank angle, or 0.0067 second of time. In run 6, spark occurs at  $40^\circ$  B.T.C., peak pressure occurs at  $1^\circ$  B.T.C., and detonation occurs at  $4^\circ$  B.T.C.; hence, the duration of the flame is about  $37^\circ$  of crank angle, or 0.0077 second of time. In addition, average pressures for run 6 are higher during the interval between spark and peak pressure, and thus the average combustion temperatures and the quantity of energy radiated should be greater. Then, in the case of run 6 the flame is in contact with the unburned charge longer, and energy is radiated from the burned charge at a higher rate. These effects should cause detonation to occur at a lower pressure. Again the reverse is observed to be true. Hence in this work the combined effect of heat transfer and radiation - as regards the unburned part of the charge, the burned part, the piston, the exhaust valve, and the cylinder walls - does not account for the observed differences in maximum permissible pressure of the end gas. Actually if these effects were zero, the maximum permissible pressure for run 6 would be even greater as compared with that of run 1.

Perhaps these differences in maximum permissible pressure can be accounted for by changes in flame speed. Flame speed is affected by every operating variable (references 2, 19, 20, and 21). As no records of the actual flame speeds for the present tests are available, it will be necessary to estimate these speeds from the indicator diagrams. By use of the assumption that the time required for combustion is given by the interval between the passage of spark and the instant of detonation, the average flame speeds will be inversely proportional to this time.



Again, if the series of runs at 800 rpm are considered, the time of burning for run 1 is 0.0067 second and increases uniformly for runs 2, 3, 4, and so forth, until a value of 0.0077 second is obtained for run 6. Let  $v$  represent the average flame speed for run 6, then  $1.2v$  will represent the average flame speed for run 1. The maximum permissible pressure for run 1 is 389 pounds per square inch absolute and increases uniformly to 497 pounds per square inch absolute for run 6. Here there is a consistent correlation between the average flame speeds and the maximum permissible pressures. Thus, the hypothesis might be formulated that increase in average flame speed causes a decrease in maximum permissible pressure.

These changes in flame speed for runs 1 to 6 were effected by changes in spark advance and compression ratio only. If the relation between flame speed and maximum permissible pressure is general, it should hold regardless of the procedure used to vary the flame speed. In run 33, for instance, the time of combustion is 0.0041 second and the average flame speed is  $1.9v$ . This increase in average flame speed, over that of run 6, was brought about by changing engine speed and compression ratio only. Here, however, the increase in flame speed has resulted in an increase in maximum permissible pressure. This fact contradicts the previous generalization on flame speed and maximum permissible pressure and, therefore, changes in flame speed alone cannot account for the observed results. These data are summarized in table XIII.

An objection might be raised to this demonstration on the ground that, in changing the engine speed (piston speed) and compression ratio, the heat transfer effects were also changed, and these effects may have operated in a manner which would prohibit any inferences being drawn regarding flame speed alone. This is not the case, however.

The contributions to temperature effects due to increase in piston speed should give a result opposite to that observed because the unburned charge in run 33 has only half as much time to give up heat to the cylinder surfaces as that of run 6 and should therefore detonate at a lower pressure. Actually, in run 33, the maximum permissible pressure is 109 pounds per square inch higher. Also, the time during which energy may be radiated from the burned charge is only half as long in the case of run 33, but the average combustion temperatures are considerably higher. Consequently, the difference in the



amount of radiated energy in either case is probably small and therefore should not contribute materially to the observed results.

Another objection might be raised on the ground that runs 1, 6, and 33 apparently have no common basis of comparison - because different compression ratios are used in each run. It should be remembered, however, that the common basis of comparison in this work is incipient detonation. Thus it can be shown that, in the case of run 6, if the compression ratio were fixed, an increase in engine speed, at constant spark advance, would bring run 6 into a nondetonating region (see fig. 7) and would therefore allow a higher pressure for incipient detonation. It can also be shown that a decrease in spark advance at constant compression ratio and engine speed would bring run 6 into a region of heavier detonation and would require a decrease in pressure for the same level of detonation. Increase in engine speed under these conditions results in an increase in flame speed, and decrease in spark advance causes a decrease in flame speed (reference 21).

Hence, under these conditions there would be a consistent correlation between flame speed and maximum permissible pressure: namely, an increase in flame speed would allow an increase in maximum permissible pressure. Such a proposition, if established as a generality, would be meaningless for, as soon as advantage were taken of the allowable change in pressure by varying the compression ratio, or inlet pressure, the original contradictory effects of flame speed would be evidenced.

The variation in residual gas content will have a small effect on maximum permissible pressure (reference 9), but these effects are of the order of experimental errors since the total weight of charge per cycle was maintained essentially constant. Therefore, since the observed effects of the present investigation cannot be entirely accounted for by such variable factors as have so far been recognized in this work, the existence of another variable must be assumed to account for them; this variable is the ignition delay. In this sense ignition delay may be said to have been isolated.

It should be emphasized that, although the foregoing discussion shows that the effects of heat transfer and flame motion are insufficient to explain the observed changes in maximum permissible pressure, the discussion in no way implies that these



effects do not influence the maximum permissible pressure in their own right. Obviously they do, and the question might be raised as to how much of the total change is due to change in delay alone. This question has no meaning, for a moment's reflection will make it clear that the delay is a function of the path of compression and this path is a function of heat transfer and flame speed as well as every other operating variable; therefore, a change in delay implies a change in one or more of these variables and there is no such thing as a change in delay alone.

### Theory of Chain Reactions as Explanation of Ignition Delay

The phenomenon of delay is probably best explained by the theory of chain reactions which, in brief, specifies that spontaneous ignition depends on two general types of reaction: chain-branching reaction conducive to explosion and its negative, chain-breaking reaction. The rates of these reactions are assumed equal prior to explosion, but, if the physical conditions favorable to explosion are augmented, the chain-branching reactions gain the ascendancy, become self-accelerating, and proceed violently forward (reference 22).

If  $P_1$  represents the minimum self-ignition pressure, then the rates of the chain-branching and chain-breaking reactions are equal up to point A. (See fig. 8.) At point A the chain-branching reactions gain the ascendancy and continue to accelerate at an ever-increasing rate until at point B the rate becomes enormous; this highly accelerated reaction is recognized as the explosion.

Little or no evidence of the events occurring between points A and B has been obtained. In the experiments of Tizard and Pye (reference 6) the only external manifestation was a slight drop in pressure, which was attributed to cooling due to heat lost to the surroundings. But the theory of chain reactions is promising, and it is worth while to use it freely even though it may require later modification.

Since an explosion is merely a matter of rate, it might be asked, in the light of the preceding discussion, what was meant by the expression "instant of explosion" used in the definitions of apparent and total delay. Thus it might be assumed that, since the chain-branching reactions had gained



the ascendancy at A, this instant represented the beginning of the explosion. This way of looking at the process is rather unnatural; the expression "instant of explosion" will therefore be taken to mean the instant when the rate of pressure rise becomes substantially infinite.

It might be pointed out that, with respect to the chain-reaction hypothesis, there is very little fundamental difference between the processes of normal burning and detonation in an engine cylinder. In normal burning the molecules are first energized by the electric spark. They then become energy-rich molecules or chain carriers and possess the property of energizing other molecules with which they come in contact, to the extent that any tendency for chain-breaking reactions to slow down the process is overwhelmed. The chemical combination, or "burning," takes place rapidly but only in the flame front where energy-rich molecules exist in abundance. Ahead of the flame front the temperature and pressure of the unburned part is rapidly rising and, as a result, energy-rich molecules are being formed at many points. But chain-breaking or "poisoning" molecules are also being formed ahead of the flame front, and these tend to retard the accumulation of energy-rich molecules. At a sufficiently high pressure and temperature the rate of formation of energy-rich molecules in the unburned part becomes so great that the chain-branching reactions rush to completion and the charge is said to detonate. This process is essentially the same as the process that takes place in the flame front, but there it is limited to a thin surface of reaction; whereas, when the unburned part of the charge detonates, the reaction takes place throughout the entire volume. The violence of detonation is due not only to the rapidity of the reaction but also to the high density of the unburned charge. This density may be six times that of the charge when spark ignition occurs, and hence the chemical energy liberated would be six times that of an equal volume burned normally in the early stages of combustion. That a sudden release of energy in the end zone is responsible for high-frequency pressure waves in the combustion chamber and the characteristic pinking sound of detonation has been clearly demonstrated by Draper and Morse (reference 23).

The experimental fact that apparent delay varies with pressure has been mentioned. It was stated as an experimental fact that the apparent delay could be shortened from  $t_1$  to  $t_2$  (fig. 9), depending on whether the compression was discontinued at  $P_1$  or  $P_2$ . According to the chain-reaction theory the reason



for the variation of apparent delay with pressure, is presumably, that the chain-branching reactions are given a greater acceleration in the time interval  $t_4$  when the average pressure is  $\frac{P_1 + P_2}{2}$  than they are given in the same interval when the average pressure is  $P_1$ .

The term "apparent delay" can be extremely ambiguous, even at a definite pressure. Thus, in figure 26, if the mixture is compressed from zero to  $P_2$  along path 1 and explodes at point C, the apparent delay will be  $t_1$ . If the mixture is compressed along path 2, the apparent delay will be increased to  $t_2$ , since pressures and temperatures are lower at any instant along path 2 between A and B. But there may also be some path 3 between zero and  $P_2$  along which the apparent delay will be zero.

These considerations lead to the following:

1. When compressed to a given pressure, a combustible mixture can have an infinite number of values of apparent delay, depending on the pressure-time path.
2. Different values of apparent delay may be obtained when compression proceeds to a given pressure even though the time of compression is the same in every case.
3. Although pressures along one pressure-time path are always equal to or higher than pressures along another path, the apparent delay of the first path may be greater than or less than that of the second path.

It is also apparent from figure 26 that the first two of these results apply to total delay, but the third result does not. For the case of total delay it can be stated that:

4. If pressures along one path are always equal to or higher than pressures along another path, the total delay of the first path will be less than that of the second.

This statement is the converse of the principle demonstrated experimentally in this report.

If the compression paths cross, it is possible to have various ignition pressures for a given value of total delay.



In figure 27 it will be observed that, for a given value  $t_1$  of total delay, ignition pressures -  $P_2$ ,  $P_3$ , or  $P_4$  - might be obtained depending on whether the compression path is OAB, OAC, or OAD. A similar demonstration can be given to show that when the compression paths cross, various ignition pressures can be obtained for a given value of apparent delay.

It would be convenient to have a definition of delay which would minimize the influence of the compression path in order that, when the pressure was given, the delay would be known. If the compression is instantaneous, delay will be a property of the explosive mixture defined by the pressure and will not depend upon past history. Let this property be called absolute delay and defined as the time interval between the instant of compression and the instant of explosion, provided the gas is instantaneously compressed.

In figure 28, if the gas is compressed instantaneously to  $P_1$  along path  $OA_1$ , the absolute delay will be the interval  $A_1B_1$ , and, as the compression is continued along the same path to  $P_2$ ,  $P_3$ , and so forth, definite values of absolute delay  $A_2B_2$ ,  $A_3B_3$ , and so forth, will be associated with each pressure.

In dealing with the relation between flame speed and delay in an engine cylinder, it is convenient to introduce the term "residual delay," defined as the value the apparent delay would have at a given pressure if the compression were discontinued at that pressure. The relation between flame speed and residual delay must be somewhat as represented in figures 29 and 30. In figure 29 the residual delay has diminished to zero before the entire charge has been consumed in the normal process of combustion, and detonation ensues; whereas, in figure 30 the residual delay has not reached zero when the normal flame completes its passage and no detonation takes place. Further amplification of this process awaits the determination and correlation of flame speeds and delay periods under actual engine conditions.



## APPENDIX E

## SUGGESTION FOR EXCHANGE OF DETONATION DATA

One of the great difficulties in detonation research is the lack of an absolute basis for the comparison of data. If the state of the charge at a definite crank angle and the indicator diagram were given, rational comparisons could be made. But such factors as compression ratio, spark advance, inlet temperature, boost pressure, and so forth are superficial yardsticks, and it is seldom, if ever, that the work of two experimenters can be compared, except in vague terms, on the basis of these quantities.

A particular instance illustrating the practice of investigators to express detonation data in terms of external operating variables is to be found in the work of Barnard (reference 14) on the detonating tendencies of various hydrocarbons. The results of these tests are shown in figures 31 and 32, which are reproduced from reference 14. Notice that an increase in engine speed at constant jacket and air temperature calls for a lower critical compression ratio in the case of triptane and di-isobutylene (fig. 31) and ethyl benzene (fig. 32). All the other fuels show an increase in critical compression ratio with engine speed. But it will be observed that, for all these fuels, increase in inlet and jacket temperature requires a decrease in critical compression ratio. This fact might be taken as evidence that temperature was the most important single factor causing detonation in these tests. As has been demonstrated, however, no conclusions of this nature can possibly be drawn from curves such as those of figures 31 and 32 because the pressure-temperature-time history of the unburned charge is unknown and cannot possibly be determined from these data.

The standard test conditions used to rate these fuels, moreover, were so inadvertently chosen that they gave anomalous results. Best power spark advance was used, the determination of which requires the location of the maximum point on a curve with a broad peak, and the procedure is therefore subject to considerable error. Since detonation is very sensitive to small changes in spark advance, it is quite possible that errors from this source are in part responsible for the anomalous behavior of certain of these fuels.



The curves of figure 33, also reproduced from reference 14, show that changes in engine speed will give results which can be only vaguely interpreted. Notice that the indicated mean effective pressure is, in general, higher at 2000 rpm than at 600 rpm for a given compression ratio. This higher value indicates that the air consumption per cycle was higher at the higher engine speed. As a result of this fact alone, peak pressures would be higher at 2000 rpm than at 600 rpm for a given compression ratio. In particular, the indicated-mean-effective-pressure curves show that, at a compression ratio of about 4, the change in indicated mean effective pressure (or pounds of air per cycle) with engine speed is small, but, as the compression ratio is increased, the change rapidly becomes significant.

Apparently then, critical compression ratios determined under these conditions may give a fair estimate of the effect of engine speed on detonation for fuels with low critical compression ratios (4 or 5), but, for fuels with high critical compression ratios (10 to 14), the method is misleading. Because the critical compression ratios for triptane, ethyl benzene, and diisobutylene are all high (above 11 at 600 rpm), considerable doubt is cast on the results for these particular fuels.

Such data may serve a useful purpose in indicating the performance of various fuels under practical operating conditions, but, as far as basic research on detonation is concerned, they are of little value. It would be of interest to study these fuels by the method suggested in the text, that is, by a study of their  $dP/dt$  records.

Another instance of a research which does not allow any fundamental interpretation is that conducted by Lee (reference 24) on the effect of engine speed and mixture temperature on detonation. Lee attributed the observed change in detonation intensity with engine speed to the change in volumetric efficiency; however, many other factors that were not accounted for contributed to the change.



## REFERENCES

1. Clark, G. L., and Thee, W. C.: Present Status of the Facts and Theories of Detonation. *Ind. and Eng. Chem.*, vol. 17, no. 12, Dec. 1925, pp. 1219-1226.
2. Withrow, Lloyd, and Boyd, T. A.: Photographic Flame Studies in the Gasoline Engine. *Ind. and Eng. Chem.*, vol. 23, no. 5, May 1931, pp. 539-547.
3. Withrow, Lloyd, and Rassweiler, Gerald M.: Slow Motion Shows Knocking and Non-Knocking Explosions. *SAE Jour.*, vol. 39, no. 2, Aug. 1936, pp. 297-303, 312.
4. Ricardo, Harry R.: Paraffin as Fuel. *The Automobile Engineer*, vol. IX, no. 2, Jan. 1919.
5. Taylor, E. S.: The Importance of Auto-Ignition Lag in Knocking. *TN No. 452, NACA*, 1933.
6. Tizard, H. T., and Pye, D. R.: Experiments on the Ignition of Gases by Sudden Compression. *Phil. Mag.*, ser. 6, vol. 44, no. 259, July 1922, pp. 79-121.
7. Serruys, Max: La Combustion détonante dans les moteurs a explosion. *Pub. Sci. et Tech. du Ministère de l'Air*, No. 103, 1937.
8. Rothrock, A. M., and Biermann, Arnold E.: The Knocking Characteristics of Fuels in Relation to Maximum Permissible Performance of Aircraft Engines. *Rep. No. 655, NACA*, 1939.
9. Taylor, E. S., Leary, W. A., and Diver, J. R.: Effect of Fuel-Air Ratio, Inlet Temperature and Exhaust Pressure on Detonation. *Rep. No. 699, NACA*, 1940.
10. Rothrock, A. M., and Spencer, R. C.: A Photographic Study of Combustion and Knock in a Spark-Ignition Engine. *Rep. No. 622, NACA*, 1938.
11. Rothrock, A. M., Spencer, R. C., and Miller, Cearcy D.: A High-Speed Motion-Picture Study of Normal Combustion, Knock, and Preignition in a Spark-Ignition Engine. *Rep. No. 704, NACA*, 1941.
12. Miller, Cearcy D.: A Study by High-Speed Photography of Combustion and Knock in a Spark-Ignition Engine. *Rep. No. 727, NACA*, 1942.



13. Fenning, R. W., and Cotton, F. T.: Experiments on the Ignition of Gases by Sudden Compression. R. & M. No. 1324, British A.R.C., 1930.
14. Barnard, D. P.: The A.P.I. Hydrocarbon Research Project. Refiner and Natural Gas. Mfr., vol. 18, no. 11, Nov. 1939, pp. 456-465.
15. Goodenough, G. A.: Principles of Thermodynamics. 4th ed., Henry Holt and Co., 1931, p. 278.
16. Reynolds, Blake, Schecter, Harry, and Taylor, E. S.: The Charging Process in a High-Speed, Single-Cylinder, Four-Stroke Engine. TN No. 675, NACA, 1939.
17. Spiers, H. M.: Technical Data on Fuel. 3d ed., British Nat. Comm., World Power Conf. (London), 1932.
18. Anon.: Exhaust Valves. The Automobile Engineer, vol XXVII, no. 360, July 1937, p. 273.
19. Marvin, Charles F., Jr., and Best, Robert D.: Flame Movement and Pressure Development in an Engine Cylinder. Rep. No. 399, NACA, 1931.
20. Schnauffer, Kurt: Engine-Cylinder Flame-Propagation Studied by New Methods. SAE Jour., vol. 34, no. 1, Jan. 1934, pp. 17-24.
21. Bouchard, C. L., Taylor, C. Fayette, and Taylor, E. S.: Variables Affecting Flame Speed in the Otto-Cycle Engine. SAE Jour., vol. 41, no. 5, Nov. 1937, pp. 514-520.
22. Lewis, Bernard, and von Elbe, Guenther: Combustion, Flames and Explosions of Gases. Univ. Press (Cambridge), 1938, pp. 2-5.
23. Draper, Charles S., and Morse, Philip M.: Acoustical Analysis of the Pressure Waves Accompanying Detonation in the Internal-Combustion Engine. Proc. Fifth Int. Cong. Appl. Mech. (Cambridge, Mass., 1938), John Wiley & Sons, Inc., 1939, pp. 727-732.
24. Lee, Dana W.: The Effects of Engine Speed and Mixture Temperature on the Knocking Characteristics of Several Fuels. TN No. 767, NACA, 1940.



Log sheet for runs to determine the effect of engine speed and spark advance on maximum permissible compression ratio. Engine  $3\frac{1}{2}$ " x  $4\frac{1}{2}$ " C.F.R., reference fuel C-12 78.9 octane, coolant temperature  $212^{\circ}\text{F}$ , dew point of inlet air less than  $-40^{\circ}\text{F}$ .

Run no.	Engine speed r.p.m.	Spark advance degrees	Brake lb.	Compression ratio	Inlet mixture temp. $^{\circ}\text{F}$	Inlet mixture pressure "Hg gauge	Exhaust pressure "Hg gauge	Fuel-air ratio	Barometer (true) "Hg	Weight air per suction stroke (dry) lb.
1	800	0	18.3	7.59	120	-5.3	-5.2	.0771	29.92	.000922
2	800	8	19.0	6.77	120	-5.2	-5.2	.0777	29.92	.000932
3	800	16	18.6	6.28	120	-5.2	-5.2	.0782	29.90	.000933
4	800	24	17.8	5.92	120	-5.2	-5.2	.0782	29.90	.000925
5	800	32	16.7	5.83	120	-5.0	-5.0	.0781	29.90	.000936
6	800	40	15.1	6.17	120	-5.2	-5.2	.0783	29.90	.000925
7	800	48	13.2	7.71	120	-4.0	-4.0	.0765	29.90	.000955
8	800	0	18.7	7.35	160	-4.3	-4.5	.0778	29.95	.000932
9	800	8	18.3	6.53	160	-4.4	-4.5	.0782	29.97	.000935
10	800	16	18.4	5.98	160	-4.4	-4.6	.0765	29.97	.000940
11	800	24	17.5	5.80	160	-4.3	-4.3	.0786	29.94	.000940
12	800	32	16.1	5.81	160	-4.5	-4.6	.0780	29.94	.000931
13	800	40	14.9	6.13	160	-4.3	-4.3	.0785	29.94	.000931
14	800	44	13.9	6.63	160	-3.9	-4.0	.0782	29.94	.000931
15	800	48	12.5	7.14	160	-3.8	-3.8	.0780	29.94	.000931
18	800	0	17.5	6.80	200	-3.7	-3.7	.0788	29.99	.000933
19	800	10	17.8	6.01	200	-3.5	-3.5	.0786	29.99	.000933
20	800	20	17.4	5.73	200	-3.5	-3.5	.0782	29.98	.000935
21	800	30	16.5	5.56	200	-3.5	-3.5	.0785	29.98	.000933
22	800	40	14.6	6.00	200	-3.4	-3.5	.0785	29.98	.000926
23	800	48	12.9	6.80	200	-2.9	-2.8	.0777	29.98	.000933
27	1600	5	18.0	8.94	120	-1.35	-1.4	.0780	29.90	.000928
29	1600	15	18.5	7.38	120	-1.35	-1.4	.0780	30.08	.000930
30	1600	25	18.0	6.80	120	-1.35	-1.4	.0765	30.10	.000925
31	1600	30	17.8	6.60	120	-0.6	-0.6	.0776	29.78	.000935
32	1600	35	16.8	6.67	120	-0.6	-0.6	.0785	29.79	.000930
33	1600	40	16.1	7.01	120	-0.6	-0.5	.0778	29.79	.000925
34	1600	45	14.6	7.78	120	-0.4	-0.3	.0775	29.78	.000934
35	1600	5	18.1	8.69	160	-0.1	-0.1	.0774	30.00	.000935
36	1600	15	18.4	7.09	160	-0.1	-0.1	.0784	30.00	.000941
37	1600	25	18.0	6.47	160	-0.1	-0.1	.0788	30.00	.000941
38	1600	30	17.0	6.39	160	-0.1	-0.1	.0783	30.00	.000935
39	1600	35	16.3	6.57	160	-0.1	-0.1	.0787	30.00	.000931
40	1600	40	15.0	6.85	160	-0.1	-0.1	.0789	30.00	.000931
41	1600	45	13.8	7.32	160	-0.1	-0.1	.0786	30.00	.000927
44	1600	5	16.8	8.59	200	+0.25	+0.25	.0789	30.05	.000933
45	1600	15	17.0	7.04	200	0.25	0.25	.0786	30.05	.000935
46	1600	25	15.9	6.27	200	0.25	0.25	.0786	30.04	.000928
47	1600	30	15.1	6.27	200	0.65	0.65	.0786	30.04	.000929
48	1600	35	14.2	6.30	200	0.75	0.75	.0786	30.04	.000933
49	1600	40	13.0	6.43	200	0.75	0.8	.0778	30.04	.000936
50	1600	45	12.0	6.72	200	0.75	0.8	.0786	30.04	.000927
56	2400	20	16.5	9.16	120	7.4	7.4	.0778	29.64	.000933
57	2400	30	15.8	7.64	120	7.6	7.6	.0778	29.64	.000933
58	2400	40	14.5	7.18	120	7.6	7.6	.0785	29.65	.000925
59	2400	50	12.5	7.70	120	7.6	7.6	.0772	29.65	.000925

14-32



TABLE II

SIGNIFICANT DATA PERTAINING TO THE UNBURNED CHARGE FOR RUNS AT INLET-MIXTURE TEMPERATURE OF 120° F

Run	Compression ratio	Spark advance (deg)	Weight of mixture per cycle (lb)	Weight of residual per cycle (lb)	Weight of charge per cycle (lb)	Percentage of residual by weight	Location of point 0 (°B.T.C.)	Charge volume at point 0 (cu ft)	Temperature of charge at point 0 (°F abs.)	Maximum permissible pressure of end gas, $P_3$ (lb/sq in. abs.)	Maximum temperature of end gas, $T_3$ (°F abs.)	Maximum relative density of end gas, $P_3/T_3$	Total delay measured from A (fig. 11) (sec)
Engine speed, 800 rpm													
1	7.59	0	0.000994	0.0000448	0.00104	4.3	50.0	0.00785	1070	389	1675	0.232	0.00425
2	6.77	8	.00101	.0000506	.00106	4.8	48.8	.00811	1090	423	1735	.244	.00360
3	6.28	16	.00101	.0000582	.00107	5.4	46.8	.00814	1080	440	1735	.248	.00305
4	5.92	24	.000998	.0000607	.00106	5.7	45.6	.00826	1110	455	1785	.255	.00330
5	5.83	32	.00101	.0000662	.00108	6.1	44.8	.00821	1080	468	1755	.266	.00300
6	6.17	40	.000998	.0000618	.00106	5.8	46.0	.00811	1085	497	1785	.278	.00255
7	7.71	48	.00103	.0000544	.00108	4.8	53.2	.00833	1095	576	1820	.316	.00215
Engine speed, 1600 rpm													
27	8.94	5	0.00100	0.0000408	0.00104	3.9	53.5	0.00788	1075	389	1680	0.232	0.00515
29	7.38	15	.00100	.0000528	.00106	5.0	50.4	.00802	1075	472	1750	.270	.00250
30	6.80	25	.000996	.0000600	.00106	5.7	49.5	.00822	1100	530	1830	.290	.00181
31	6.60	30	.00101	.0000671	.00107	6.2	49.5	.00835	1100	555	1845	.301	.00178
32	6.67	35	.00100	.0000673	.00107	6.3	50.0	.00838	1110	571	1870	.305	.00178
a 33	7.01	40	.000998	.0000641	.00106	6.0	51.0	.00834	1115	606	1900	.319	.00183
34	7.78	45	.00101	.0000587	.00107	5.5	53.2	.00830	1100	635	1895	.335	.00145
Engine speed, 2400 rpm													
56	9.16	20	0.00101	0.0000583	0.00106	5.6	55.2	0.00811	1085	516	1795	0.288	0.00242
57	7.64	30	.00101	.0000715	.00108	6.6	52.8	.00829	1090	540	1815	.298	.00172
58	7.18	40	.000998	.0000787	.00108	7.3	49.6	.00801	1050	571	1805	.316	.00139
a 59	7.70	50	.000997	.0000756	.00107	7.1	51.2	.00800	1060	624	1830	.341	.00147

<sup>a</sup> It is believed that detonation occurred slightly before peak pressure in these runs, but the  $dp/dt$  records were fogged and the instant of detonation could not be determined accurately.



TABLE III

## TEMPERATURE OF THE UNBURNED CHARGE AT VARIOUS CRANK ANGLES FOR RUN 27

[Firing run; high-speed C F R engine; engine speed, 1600 rpm; compression ratio, 8.94; spark advance, 5°; fuel-air ratio, 0.0780; inlet-mixture temperature, 120° F; residual content, 4.6 percent; clearance volume, 0.00272 cu ft; barometer, 14.7 lb/sq in. (true); indicator springs: heavy, 150 lb; light, 5 lb; coolant temperature, 212° F]

Crank angle, $\theta$ (° B.T.C.)	Pressure, $P_{x1}$ (lb/sq in. abs.)	Cylinder volume, $V_x$ (cu ft)	Weight of charge, $w$ (lb)	Specific volume of charge, $V$ (cu ft/lb)	Indicated temperature, $T_{x1}$ (°F abs.)	Adiabatic temperature, $T_{x2}$ (°F abs.)	Adiabatic temperature, $T_{x3}$ (°F abs.)
100	19.5	0.01658	0.001048	15.8	873	873	873
80	27.1	.01283	.001048	12.23	939	945	947
60	43.2	.00903	.001048	8.61	1055	1055	1057
40	77.7	.00575	.001048	5.48	1206	1207	1208
20	144.5	.00351	.001048	3.345	1380	1384	1390
10	182.5	.00292	.001048	2.785	1442	1457	1463
5	197.0	.00277	.001048	2.645	1478	1481	1484
0	206.5	-----	-----	-----	-----	1496	-----
-20	256	-----	-----	-----	-----	1565	-----
Peak	389	-----	-----	-----	-----	1705	-----

TABLE IV

## TEMPERATURE OF THE UNBURNED CHARGE AT VARIOUS CRANK ANGLES FOR RUN 73

[Nonfiring run, fuel-air mixture; high-speed C F R engine; engine speed, 1600 rpm; compression ratio, 6.79; fuel-air ratio, 0.0795; inlet-mixture temperature, 117° F; clearance volume, 0.00373 cu ft; barometer, 14.6 lb/sq in. (true); indicator spring, 50 lb; coolant temperature, 212° F]

Crank angle, $\theta$ (° B.T.C.)	Pressure, $P_{x1}$ (lb/sq in. abs.)	Cylinder volume, $V_x$ (cu ft)	Weight of charge, $w$ (lb)	Specific volume of charge, $V$ (cu ft/lb)	Indicated temperature, $T_{x1}$ (°F abs.)	Adiabatic temperature, $T_{x2}$ (°F abs.)	Adiabatic temperature, $T_{x3}$ (°F abs.)
100	18.6	0.01759	0.00130	13.53	717	717	717
80	25.6	.01384	.00130	10.65	774	782	785
60	38.6	.01004	.00130	7.73	850	876	886
40	66.1	.00676	.00130	5.20	980	1011	1022
20	110.6	.00452	.00130	3.48	1098	1159	1182
10	132.1	.00393	.00130	3.02	1137	1214	1242
0	145.6	.00373	.00130	2.87	1191	1245	1264

TABLE V

## TEMPERATURE AND PRESSURE OF THE UNBURNED CHARGE AT VARIOUS CRANK ANGLES FOR RUN 76

[Nonfiring run, fuel-air mixture; high-speed C F R engine; engine speed, 1600 rpm; compression ratio, 6.79; fuel-air ratio, 0.0796; inlet-mixture temperature, 123° F; clearance volume, 0.00373 cu ft; barometer, 14.8 lb/sq in. (true); indicator spring, 50 lb; coolant temperature, 212° F]

Crank angle, $\theta$ (° B.T.C.)	Pressure, $P_{x1}$ (lb/sq in. abs.)	Cylinder volume, $V_x$ (cu ft)	Weight of charge, $w$ (lb)	Specific volume of charge, $V$ (cu ft/lb)	Indicated temperature, $T_{x1}$ (°F abs.)	Adiabatic temperature, $T_{x2}$ (°F abs.)	Adiabatic temperature, $T_{x3}$ (°F abs.)	Adiabatic pressure, $P_{x3}$ (lb/sq in. abs.)
Values computed from 100° B.T.C.								
100	20.3	0.01759	0.001295	13.58	785	785	785	20.3
80	27.6	.01384	.001295	10.69	841	853	859	28.15
60	40.3	.01004	.001295	7.76	891	945	967	43.7
40	67.8	.00676	.001295	5.22	1010	1086	1115	74.9
20	113.3	.00452	.001295	3.49	1128	1241	1285	129.0
10	136.8	.00393	.001295	3.035	1182	1303	1348	155.6
0	146.3	.00373	.001295	2.88	1201	1327	1372	167.0
Values computed from 40° B.T.C.								
40	67.8	.00676	.001295	5.22	1010	1010	1010	67.8
20	113.3	.00452	.001295	3.49	1128	1157	1166	117.1
10	136.8	.00393	.001295	3.035	1182	1215	1225	141.5
0	146.3	.00373	.001295	2.88	1201	1237	1249	152.0



TABLE VI.- TEMPERATURE OF END GAS COMPUTED FROM VARIOUS POINTS ON THE COMPRESSION STROKE

FOR RUN 5 OF REFERENCE 9

[Firing run; low-speed C F R engine; engine speed, 1200 rpm; compression ratio, 6.88; spark advance, 30°; fuel-air ratio, 0.0812; inlet-mixture temperature, 200° F; residual content, 5.6 percent; clearance volume, 0.00369 cu ft; barometer, 14.8 lb/sq in. (true); indicator springs: heavy, 150 lb; light, 5 lb; coolant temperature, 211° F]

Crank angle, $\theta$ (° B.T.C.)	Pressure, $P_{x1}$ (lb/sq in. abs.)	Cylinder volume, $V_x$ (cu ft)	Weight of charge, $w$ (lb)	Specific volume of charge, $V$ (cu ft/lb)	Indicated temperature, $T_{x1}$ (° F abs.)	Maximum end-gas temperature, $T_{x2}$ (° F abs.)
146	14.8	0.02382	0.001158	20.58	863	1957
100	21.25	.01755	.001158	15.15	912	1907
30	98.8	.00544	.001158	4.70	1316	1924

TABLE VII.- TEMPERATURE OF END GAS COMPUTED FROM VARIOUS POINTS ON THE COMPRESSION STROKE

FOR RUN 37 OF REFERENCE 9

[Firing run; low-speed C F R engine; engine speed, 1200 rpm; compression ratio, 7.51; spark advance, 30°; fuel-air ratio, 0.0785; inlet-mixture temperature, 120° F; residual content, 5 percent; clearance volume, 0.003325 cu ft; barometer, 14.85 lb/sq in. (true); indicator springs: heavy, 150 lb; light, 5 lb; coolant temperature, 211° F]

Crank angle, $\theta$ (° B.T.C.)	Pressure, $P_{x1}$ (lb/sq in. abs.)	Cylinder volume, $V_x$ (cu ft)	Weight of charge, $w$ (lb)	Specific volume of charge, $V$ (cu ft/lb)	Indicated temperature, $T_{x1}$ (° F abs.)	Maximum end-gas temperature, $T_{x2}$ (° F abs.)
146	14.85	0.02345	0.00123	19.06	803	1888
100	22.35	.01719	.00123	13.97	885	1883
30	109.4	.005075	.00123	4.125	1280	1888

TABLE VIII.- TEMPERATURE OF END GAS COMPUTED FROM VARIOUS POINTS ON THE COMPRESSION STROKE

FOR RUN 51 OF REFERENCE 9

[Firing run; low-speed C F R engine; engine speed, 1200 rpm; compression ratio, 7.70; spark advance, 30°; fuel-air ratio, 0.0782; inlet-mixture temperature, 80° F; residual content, 4.8 percent; clearance volume, 0.003232 cu ft; barometer, 14.8 lb/sq in. (true); indicator springs: heavy, 150 lb; light, 5 lb; coolant temperature, 211° F]

Crank angle $\theta$ (° B.T.C.)	Pressure, $P_{x1}$ (lb/sq in. abs.)	Cylinder volume, $V_x$ (cu ft)	Weight of charge, $w$ (lb)	Specific volume of charge, $V$ (cu ft/lb)	Indicated temperature, $T_{x1}$ (° F abs.)	Maximum end-gas temperature, $T_{x2}$ (° F abs.)
146	14.8	0.02336	0.001268	18.42	773	1867
100	22.3	.01709	.001268	13.48	851	1859
30	114.6	.00498	.001268	3.93	1276	1893

TABLE IX.- TEMPERATURE AND PRESSURE OF THE UNBURNED CHARGE AT VARIOUS CRANK ANGLES FOR RUN 77a

[Nonfiring run, dry air only; high-speed C.F.R. engine; engine speed, 1600 rpm; compression ratio, 6.79; inlet-air temperature, 126° F; clearance volume, 0.00373 cu ft; barometer, 14.8 lb/sq in. (true); indicator spring, 50 lb; coolant temperature, 212° F]

Crank angle, $\theta$ (° B.T.C.)	Pressure, $P_{x1}$ (lb/sq in. abs.)	Cylinder volume, $V_x$ (cu ft)	Weight of charge, $w$ (lb)	Specific volume of charge, $V$ (cu ft/lb)	Indicated temperature, $T_{x1}$ (° F abs.)	Adiabatic temperature, $T_{x2}$ (° F abs.)	Adiabatic temperature, $T_{x3}$ (° F abs.)	Adiabatic pressure, $P_{x3}$ (lb/sq in. abs.)
100	20.3	0.01759	0.00125	14.15	776	776	776	20.3
80	28.3	.01384	.00125	11.08	847	850	852	28.35
60	43.8	.01004	.00125	8.04	950	960	963	43.97
40	74.3	.00676	.00125	5.41	1085	1109	1109	75.77
20	126.3	.00452	.00125	3.62	1233	1278	1293	131.7
10	152.3	.00393	.00125	3.145	1293	1343	1357	158.7
0	162.3	.00373	.00125	2.985	1310	1366	1385	171.7



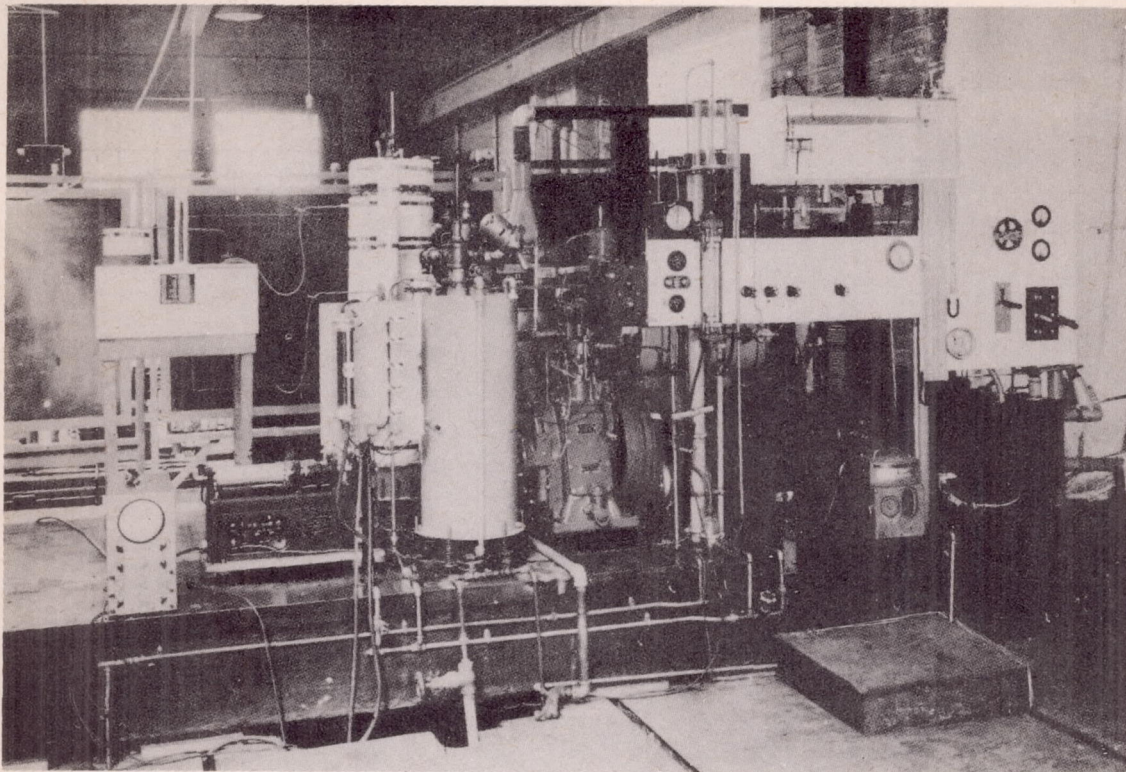
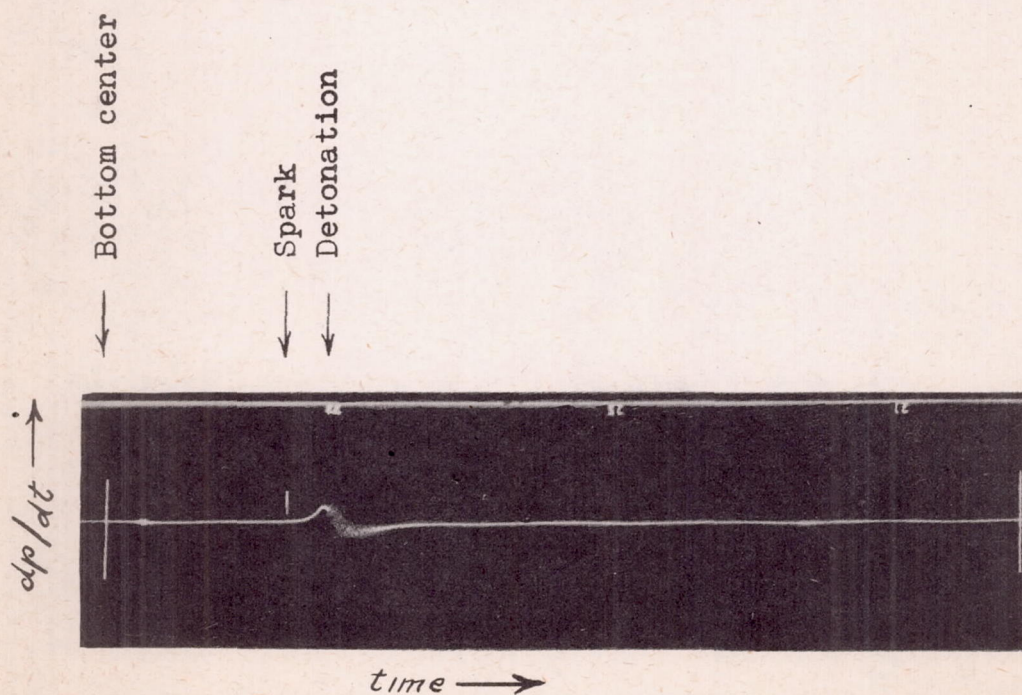


Figure 1.- Apparatus used in tests.

Figure 12. - Specimen  $\frac{dp}{dt}$  record for moderate detonation.



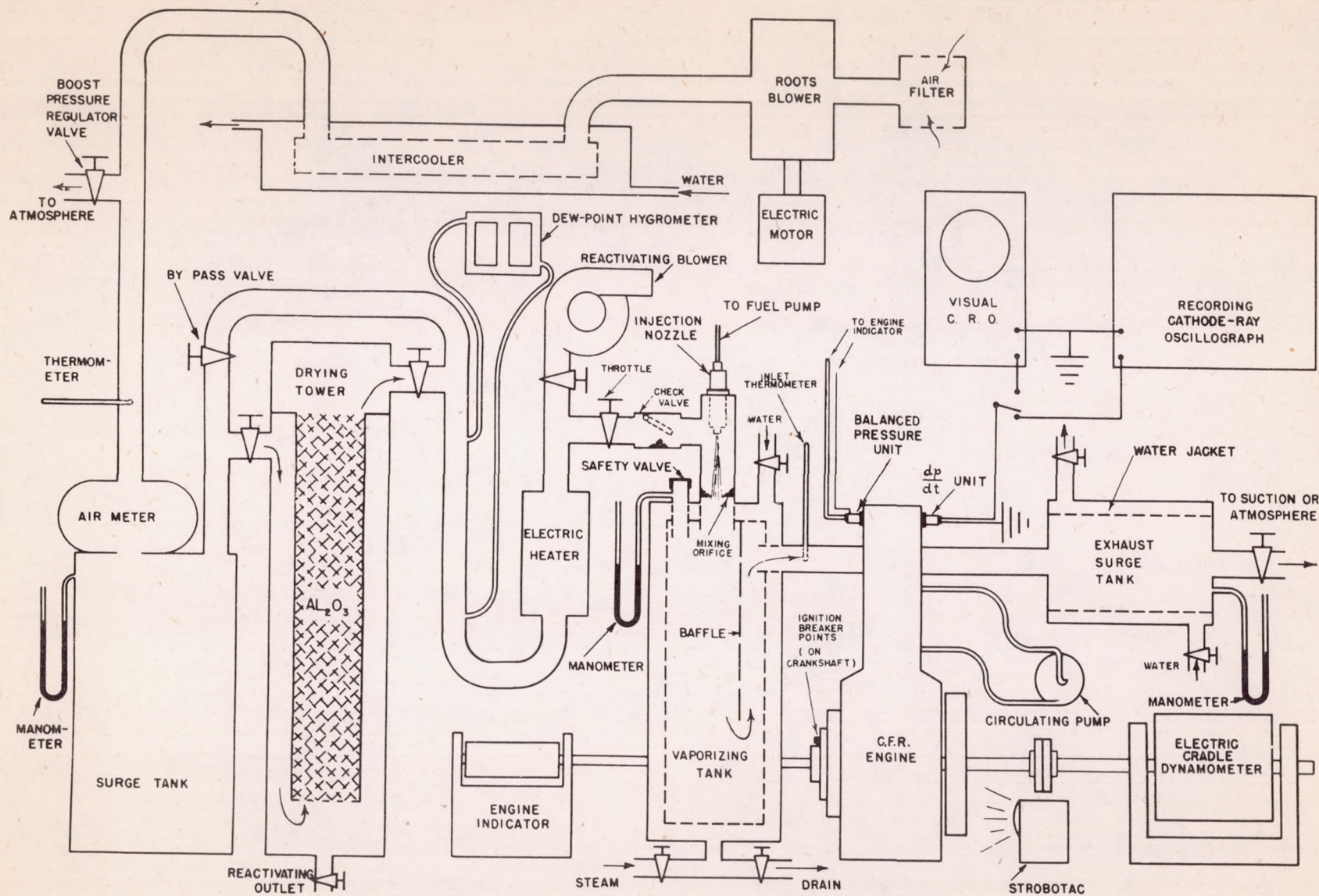


Figure 2. - Schematic diagram of apparatus.



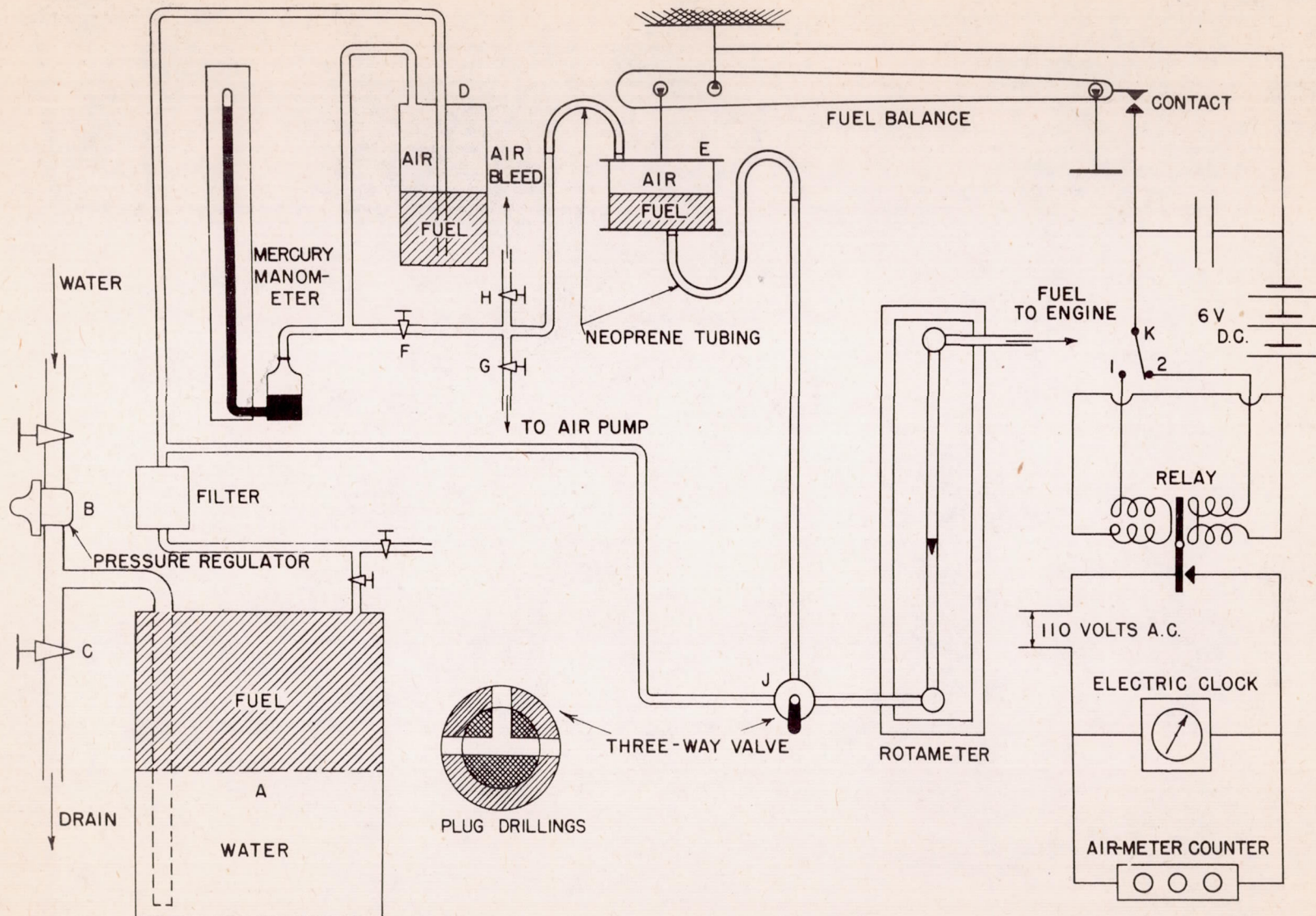


Figure 3. - Schematic diagram of fuel system.



Figure 4.- The effect of spark advance on the shape of the indicator diagram. Constant incipient detonation; engine speed, 800 rpm; other operating conditions as in table I. Maximum permissible pressure is indicated by crosses in runs 6 and 7. Numbers at the peak indicate the crank angle interval between top center and peak pressure. Spark ignition occurs at 8.

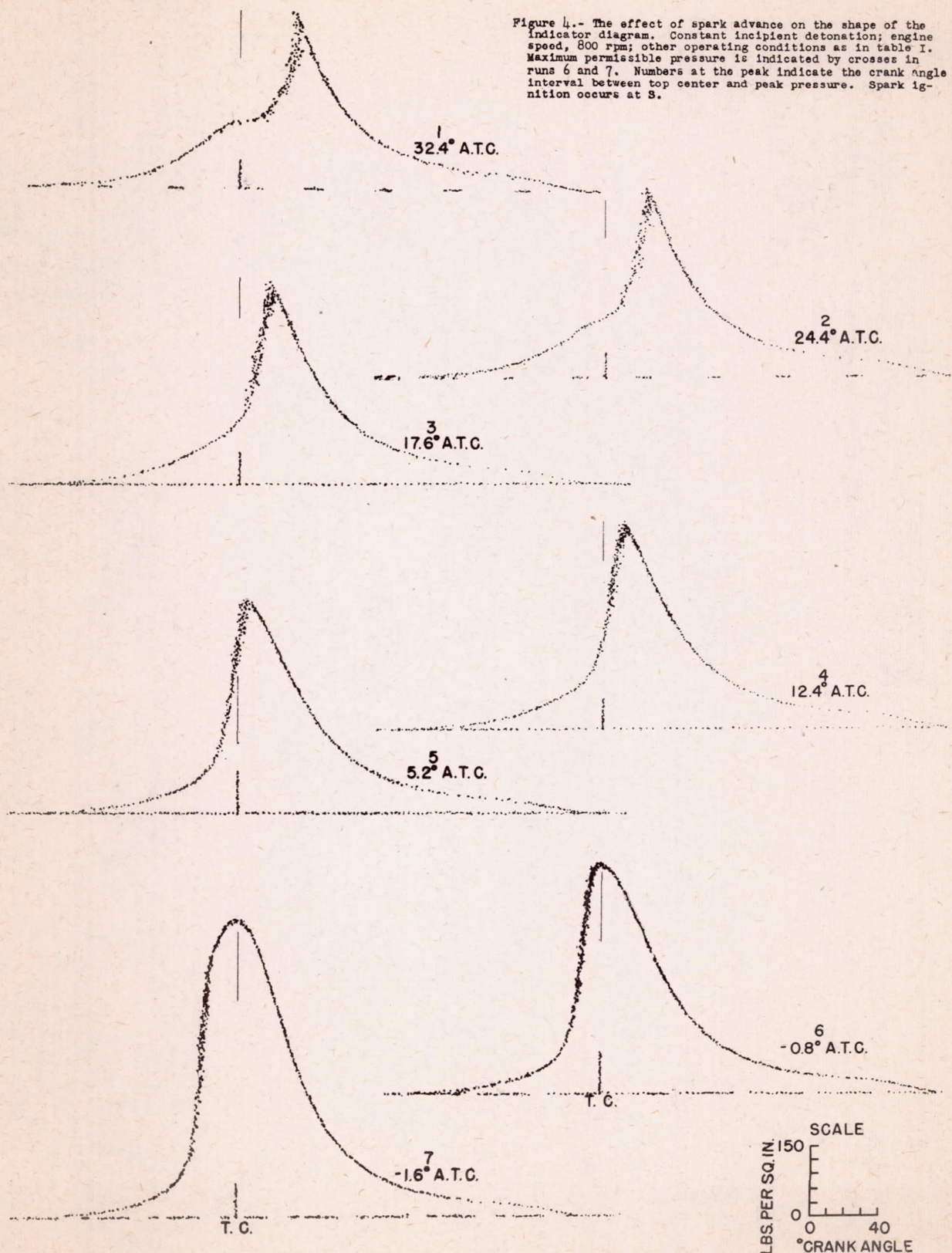




Figure 5.- The effect of spark advance on the shape of the indicator diagram. Constant incipient detonation; engine speed, 1600 rpm; other operating conditions as in table I. Maximum permissible pressure is indicated by a cross in run 34. Numbers at the peak indicate the crank angle interval between top center and peak pressure. Spark ignition occurs at S.

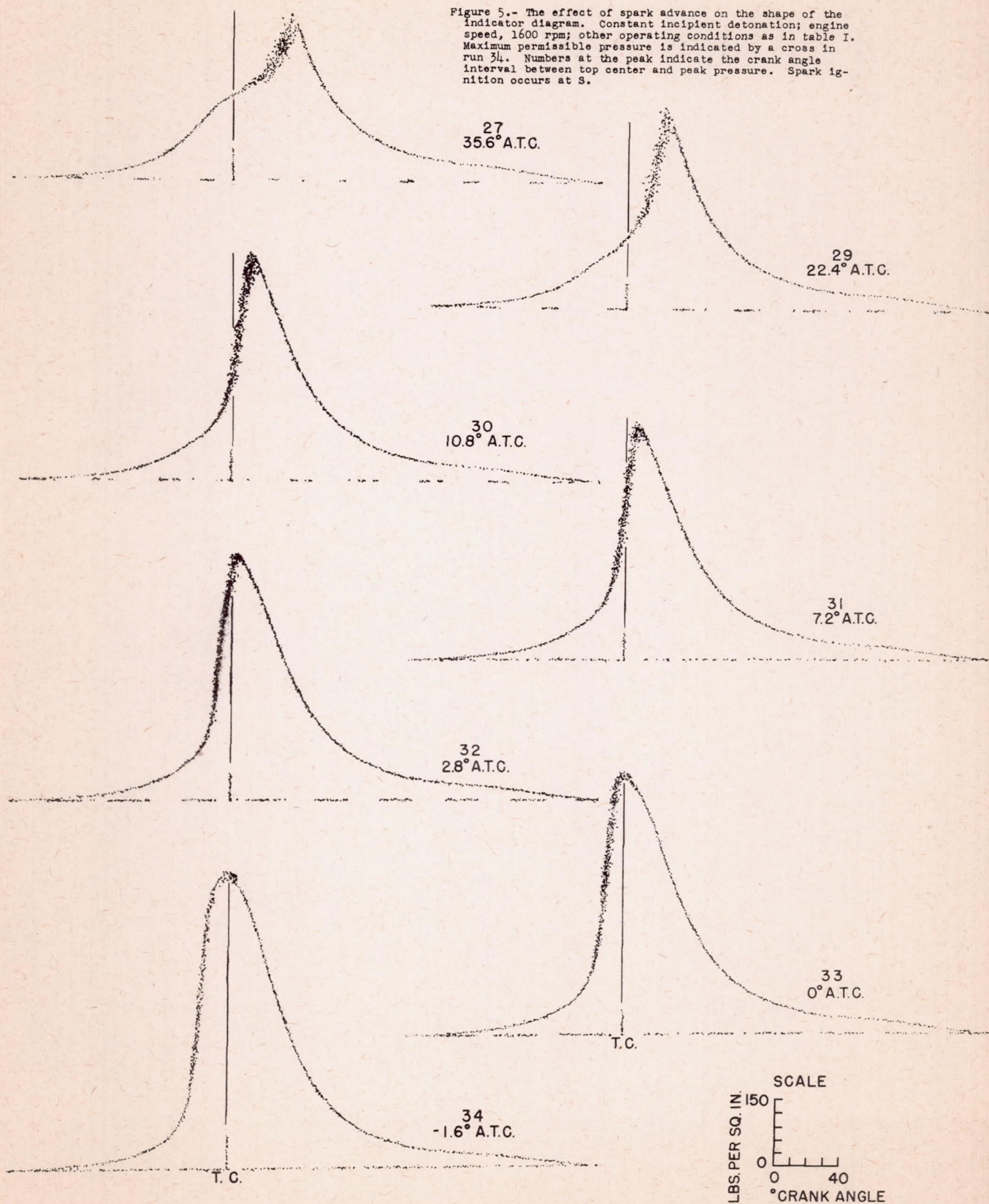
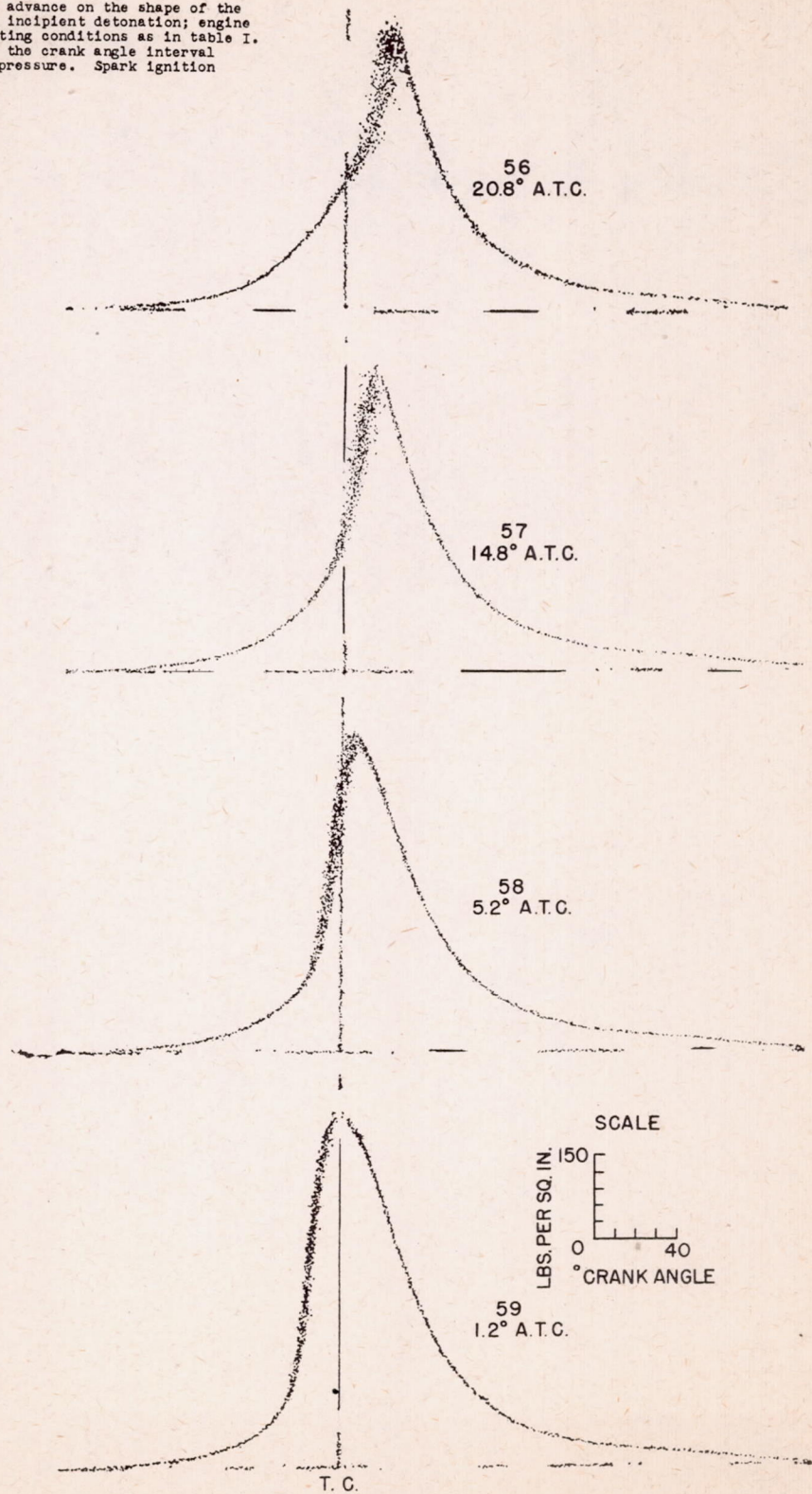




Figure 6.- The effect of spark advance on the shape of the indicator diagram. Constant incipient detonation; engine speed, 2400 rpm; other operating conditions as in table I. Numbers at the peak indicate the crank angle interval between top center and peak pressure. Spark ignition occurs at S.





Engine R P M

x 800

o 1600

△ 2400

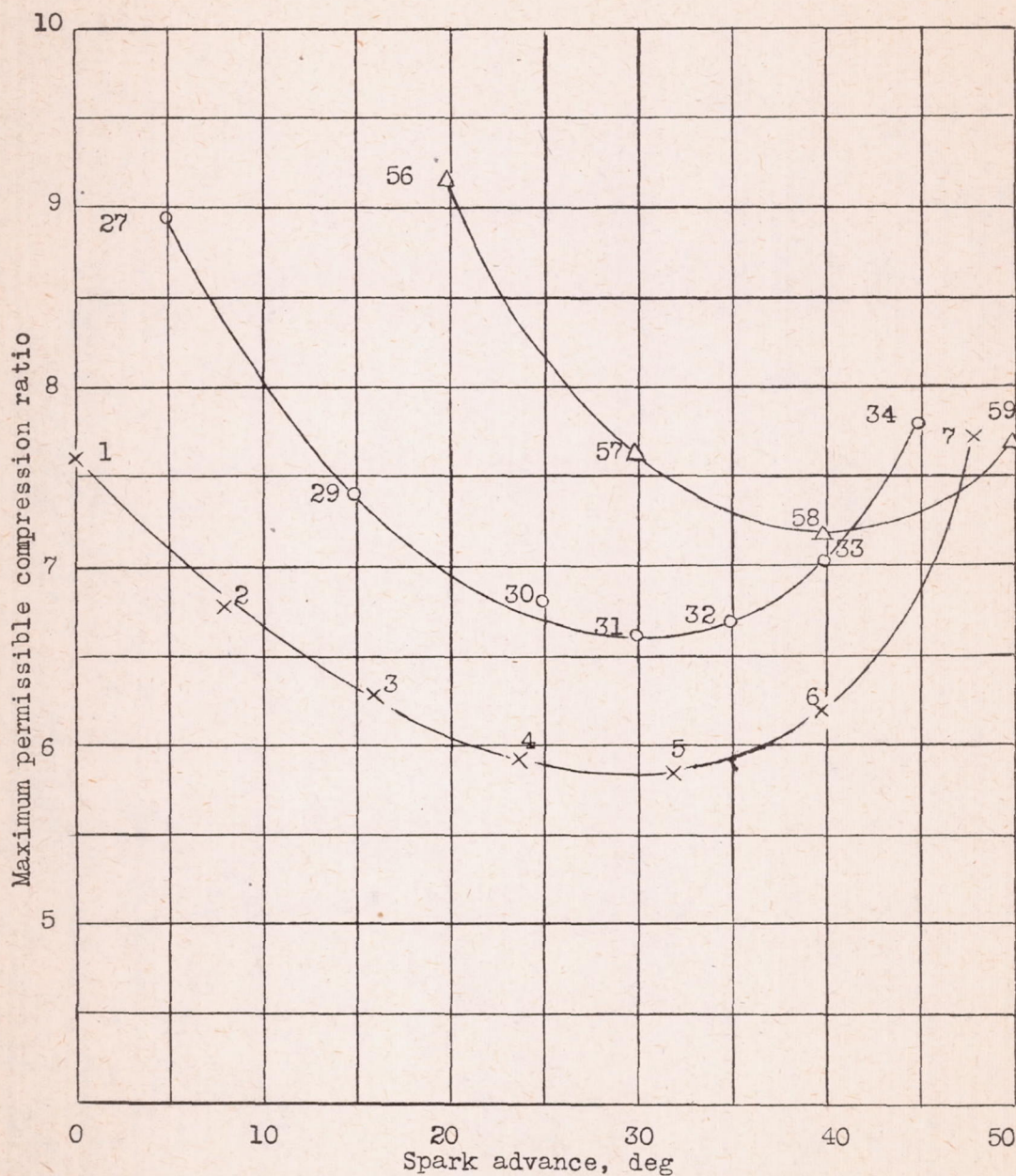


Figure 7--Effect of spark advance and engine speed on maximum permissible compression ratio. C.F.R. engine; inlet mixture temperature, 120°F; fuel 78.9 octane. Numbers on points correspond to runs listed in table 1.



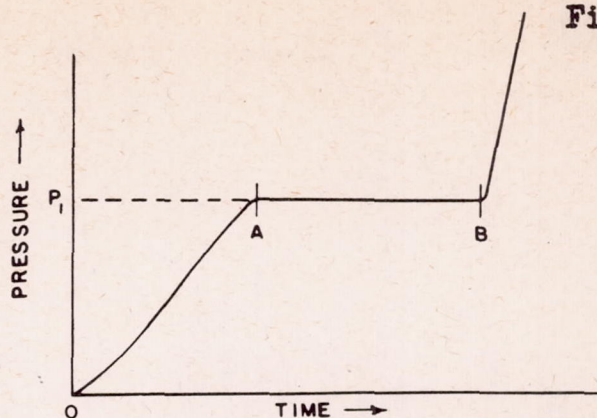


Figure 8. - Pressure-time curve for sudden compression of fuel-air mixture showing apparent delay.

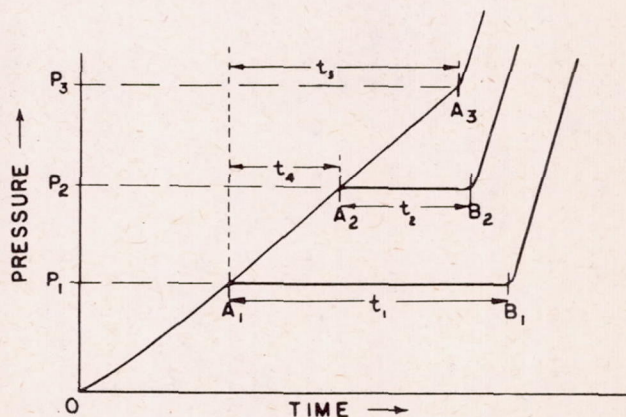


Figure 9. - Pressure-time curves for sudden compression of fuel-air mixture showing how delay varies with pressure.

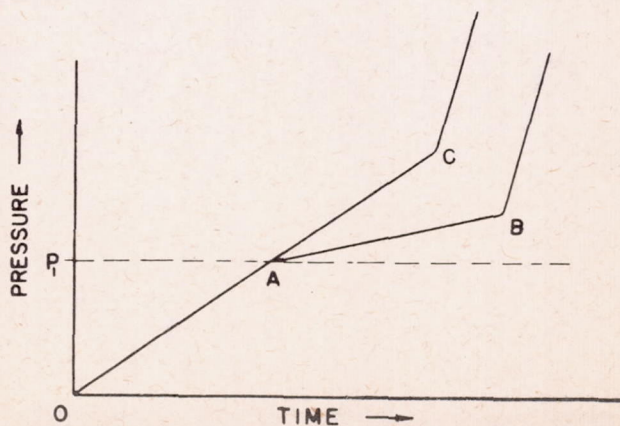


Figure 10. - Effect of change in total delay on the self-ignition pressure of a combustible mixture when compressed continuously along two paths which do not cross above  $P_1$ .



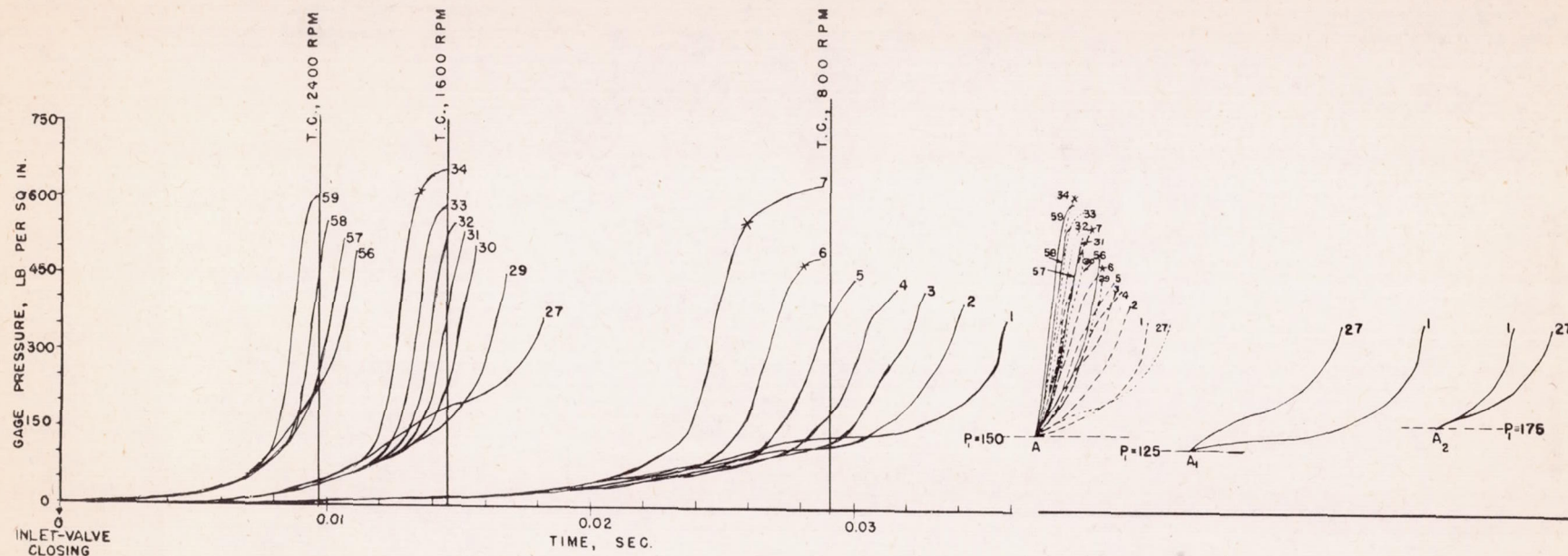


Figure 11. - Pressure-time indicator diagrams for runs at constant incipient detonation. Only the lines of rising pressure are shown. Numbers on curves correspond to runs listed in table I. Maximum permissible pressure is indicated by crosses in runs 6, 7, and 34.



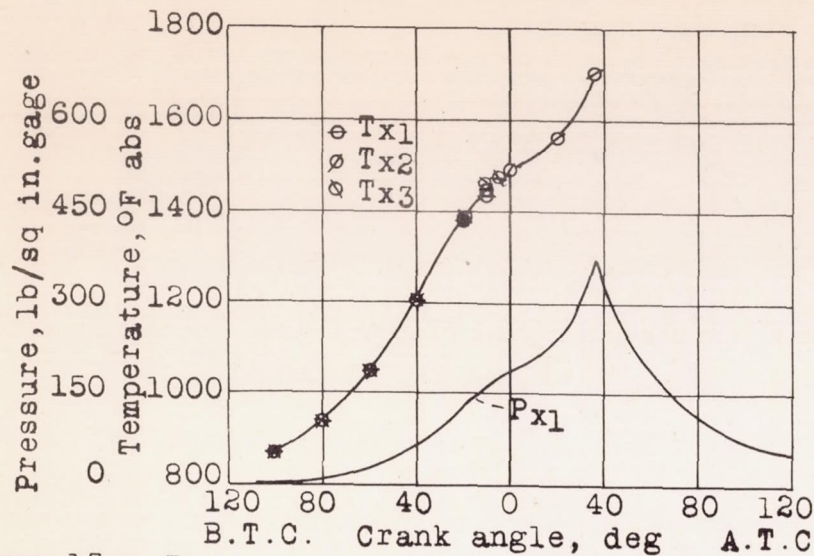


Figure 13.- Temperature of the unburned charge and cylinder pressures at various crank angles, run 27. See table III.

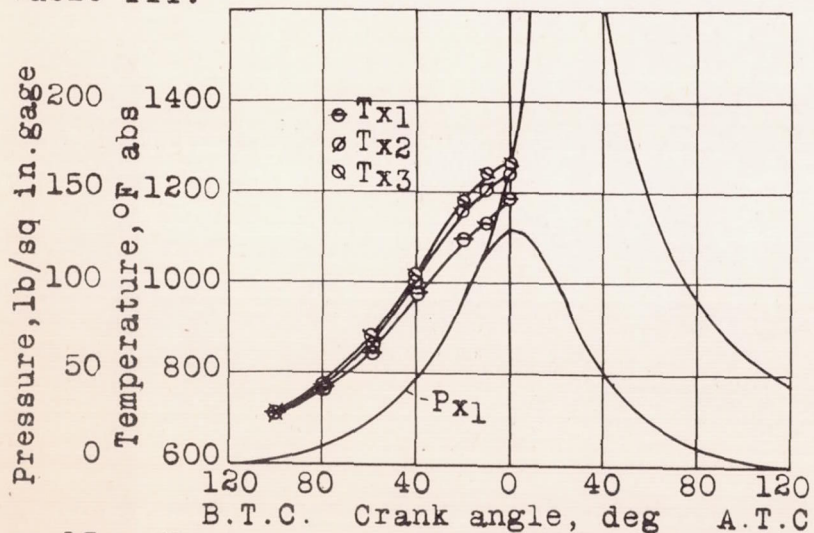


Figure 15.- Temperature and pressure of the unburned charge at various crank angles, run 73. See table IV.

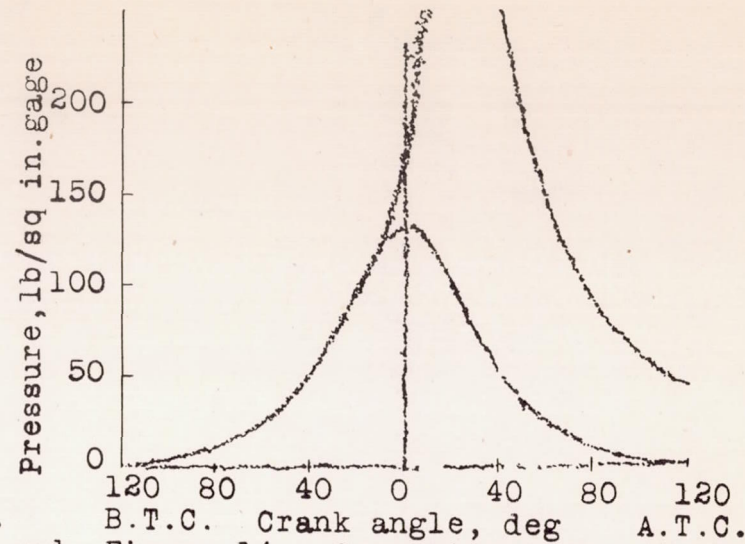


Figure 14.- Composite indicator diagram for run 73.

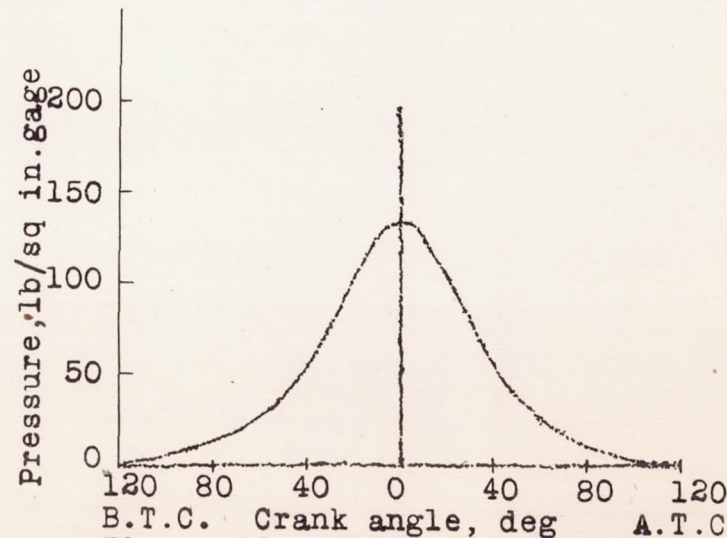


Figure 16.- Indicator diagram for run 76. See table V.

NACA

Figs. 13, 14, 15, 16



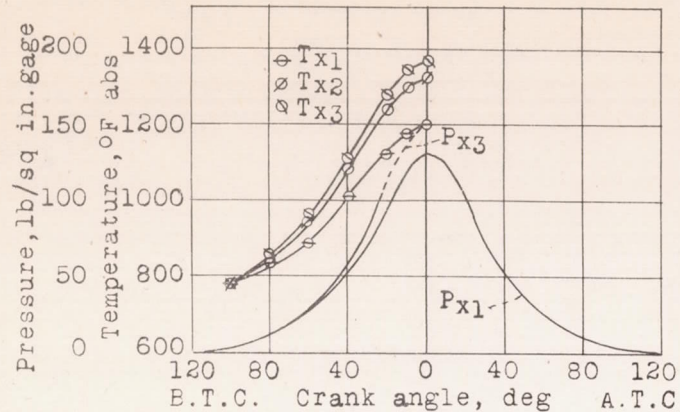


Figure 17.- Temperature and pressure of the unburned charge at various crank angles, computed from 100° B.T.C., run 76. See table V.

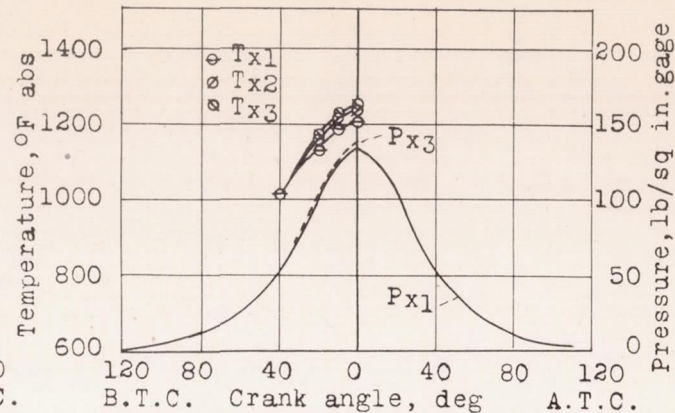


Figure 18.- Temperature and pressure of the unburned charge at various crank angles, computed from 40° B.T.C., run 76. See table V.

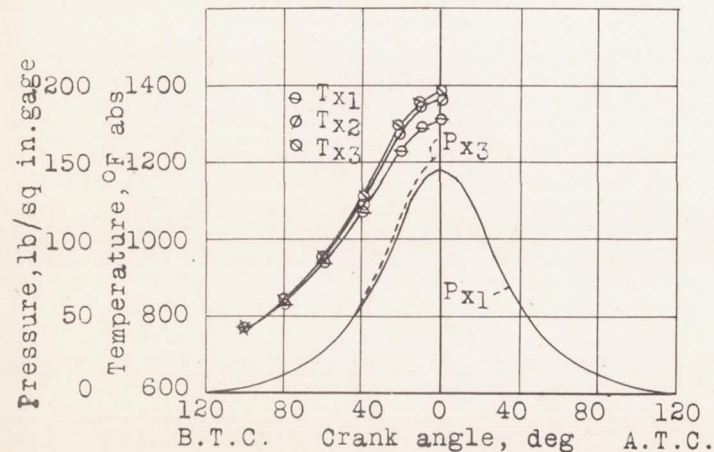


Figure 19.- Temperature and pressure of the unburned charge at various crank angles, run 77a. See table IX.

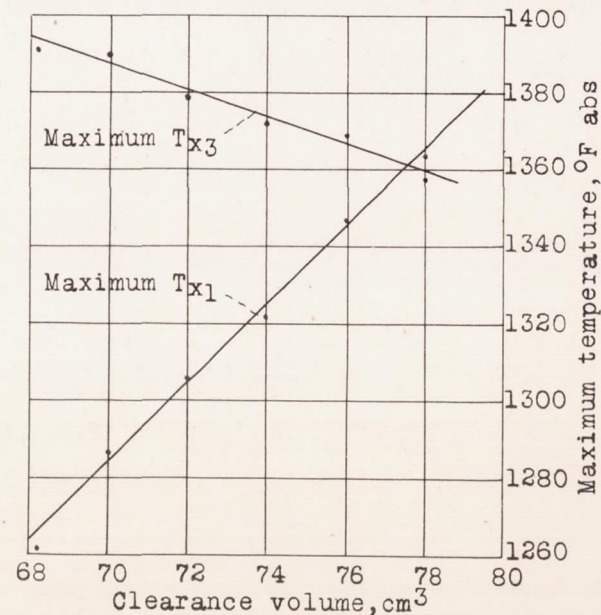


Figure 21.- Effect of clearance-volume errors on maximum values of indicated and adiabatic temperatures, run 77a.



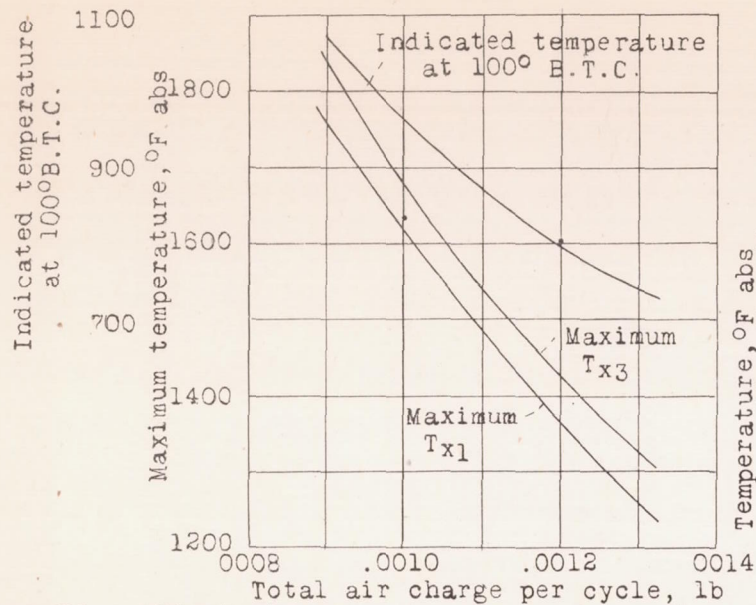


Figure 20.- Effect of errors in air measurement on maximum values of indicated and adiabatic temperatures and indicated temperature at 100° B.T.C., run 77a.

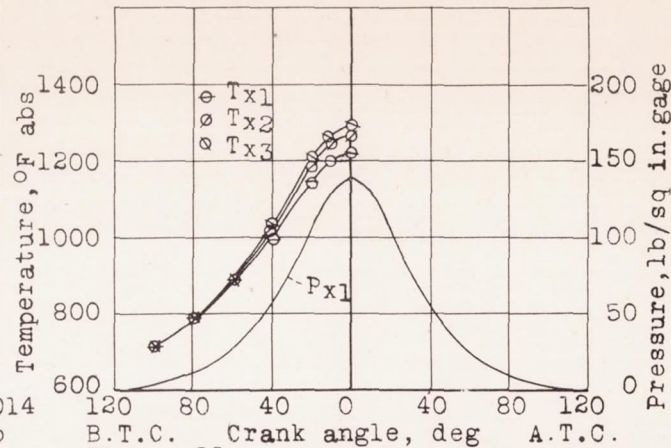


Figure 22.- Temperature and pressure of the unburned charge at various crank angles, run 78. See table X.

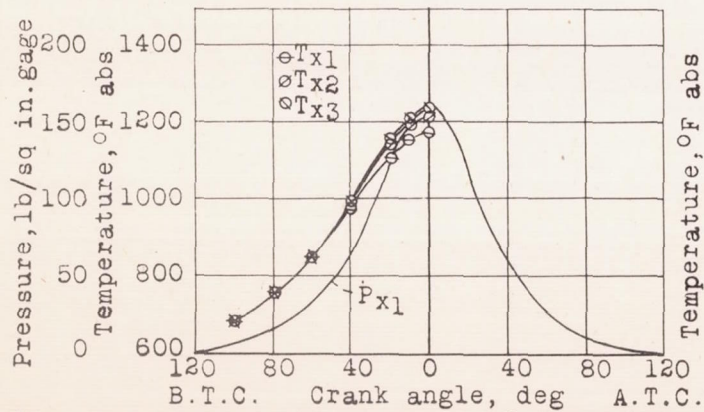


Figure 23.- Temperature and pressure of the unburned charge at various crank angles, run 79. See table XI.

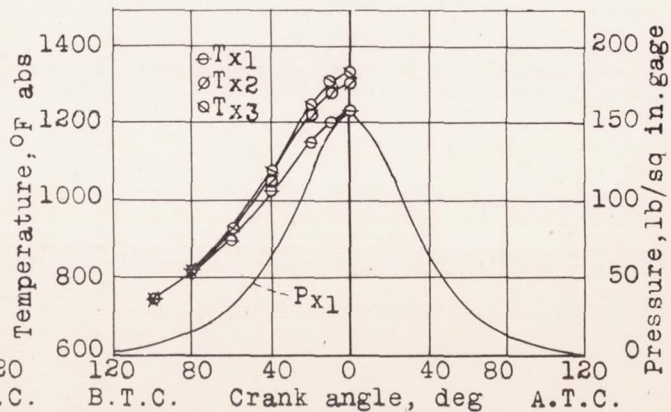


Figure 24.- Temperature and pressure of the unburned charge at various crank angles, run 80. See table XII.



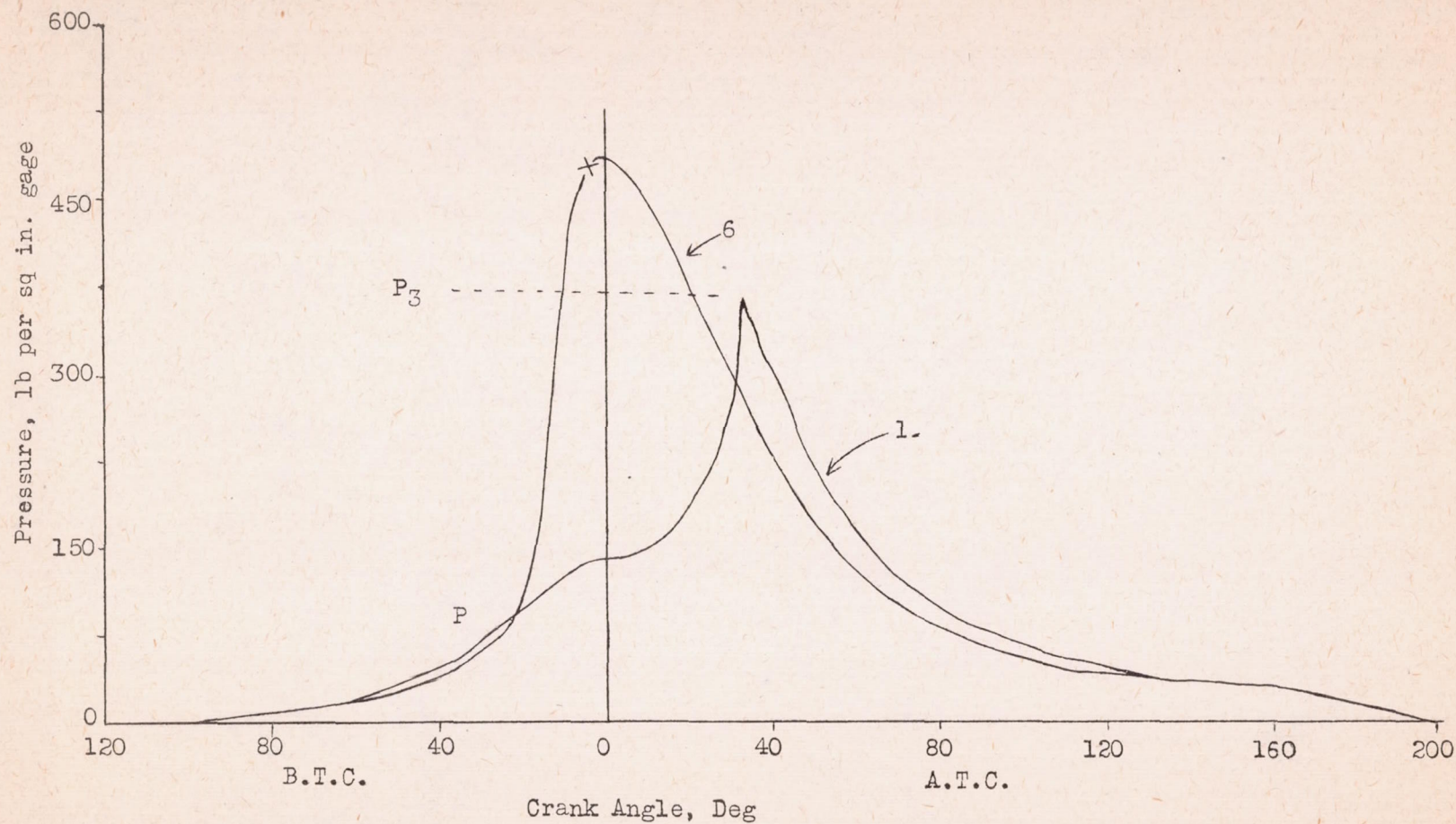


Figure 25- Comparison of indicator diagrams for runs 1 and 6. Maximum permissible pressure is indicated by a cross in run 6.



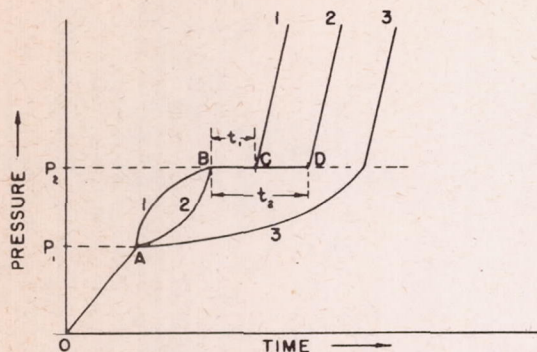


Figure 26. - Effect of path of compression on the value of apparent delay at a given pressure.

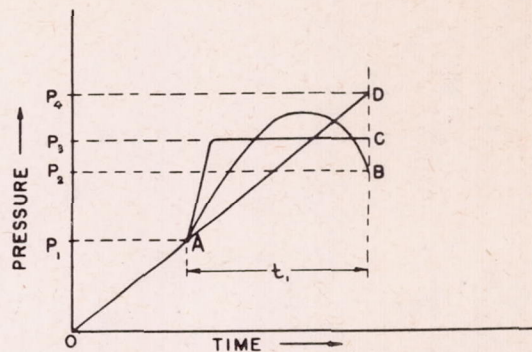


Figure 27. - Effect of path of compression as self-ignition pressure for a constant value of total delay.

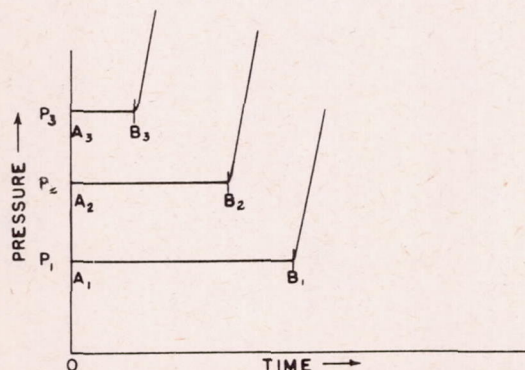


Figure 28. - Pressure-time curves for instantaneous compression of fuel-air mixture showing how absolute delay varies with pressure.

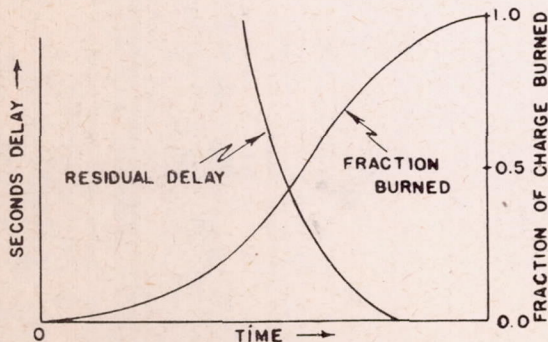


Figure 29. - Effect of flame propagation on residual delay in a detonating engine.

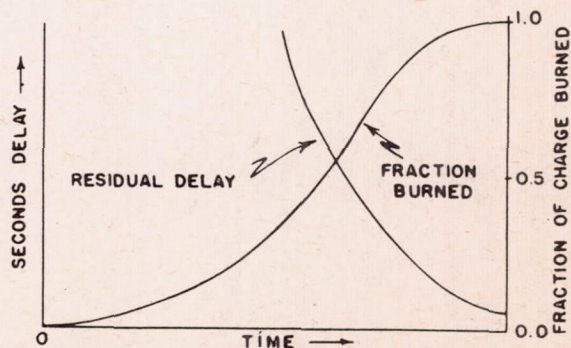


Figure 30. - Effect of flame propagation on residual delay in a non-detonating engine.



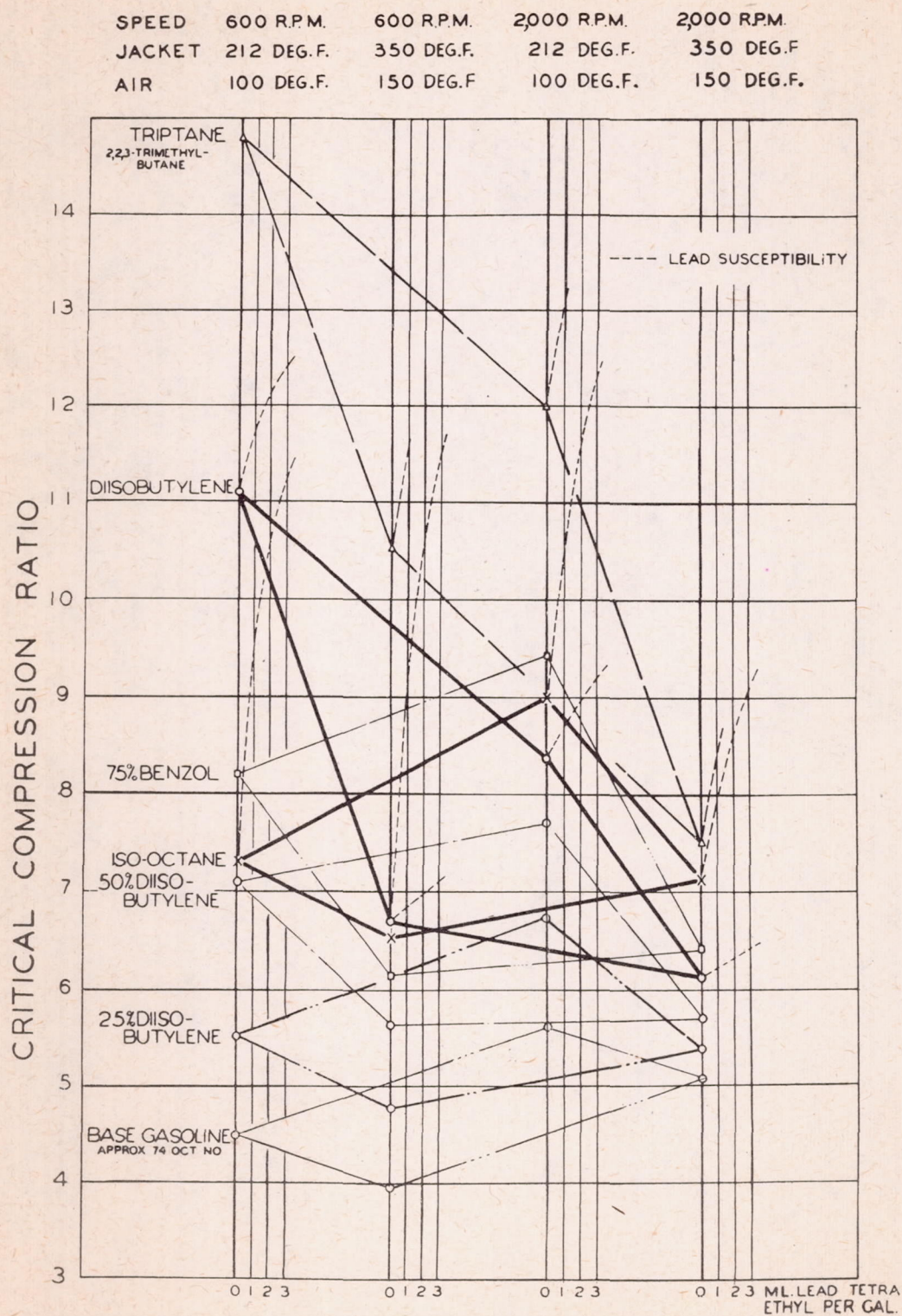


Fig. 31.-Variation in critical compression ratio of six fuels for four standard test conditions (reference 14).



SPEED	600 R.P.M.	600 R.P.M.	2000 R.P.M.	2000 R.P.M.
JACKET	212 DEG.F.	350 DEG.F.	212 DEG.F.	350 DEG.F.
AIR	100 DEG.F.	150 DEG.F.	100 DEG.F.	150 DEG.F.

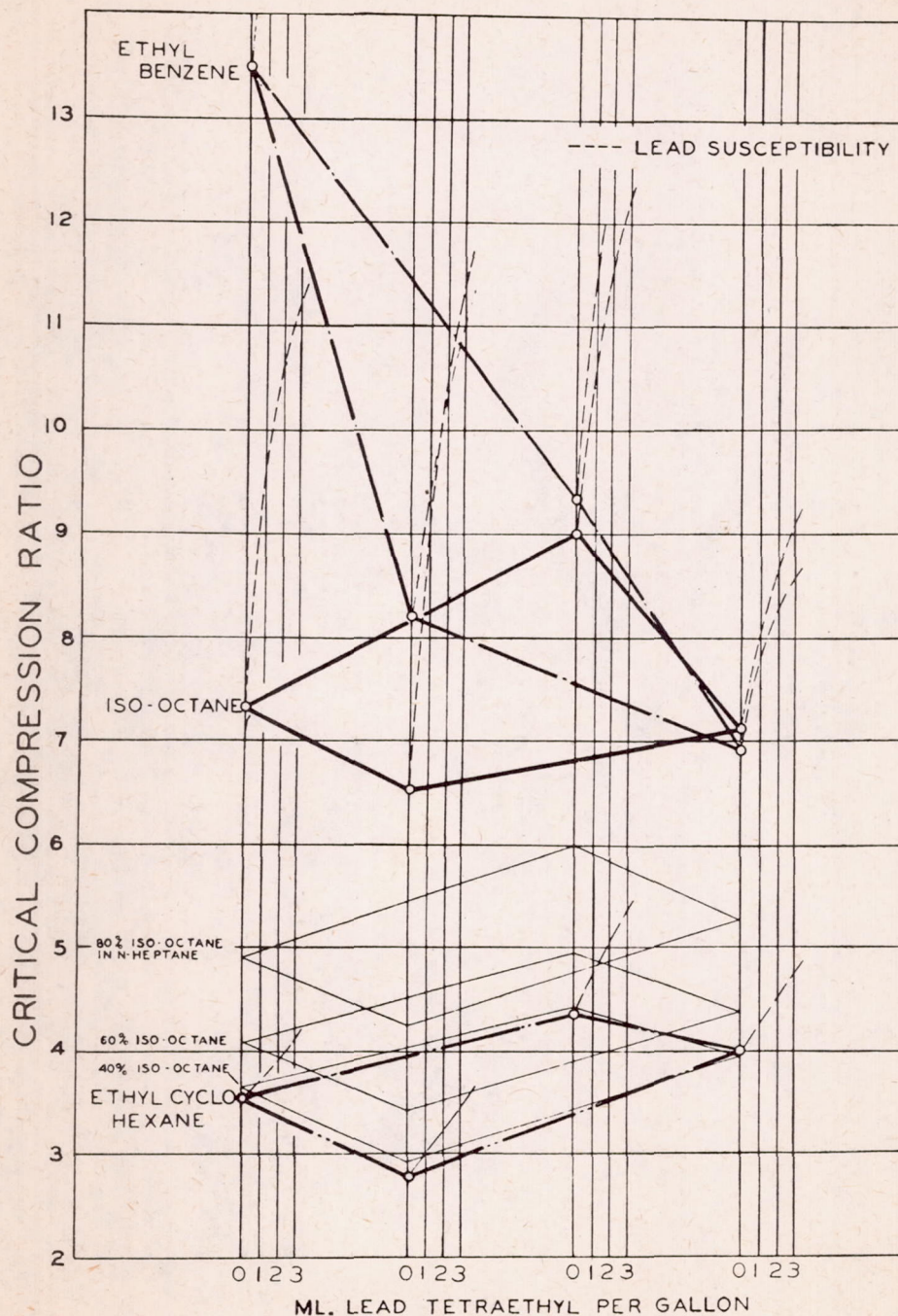


Fig. 32.-Variation in critical compression ratio for four standard test conditions, for ethyl benzene, ethyl cyclohexane, and iso-octane (2, 3, 4-trimethylpentane) (reference 14).



- 600 rpm, 212 °F jacket, 100 °F air  
△ 600 rpm, 350 °F jacket, 150 °F air  
+ 2,000 rpm, 212 °F jacket, 100 °F air  
□ 2,000 rpm, 350 °F jacket, 150 °F air

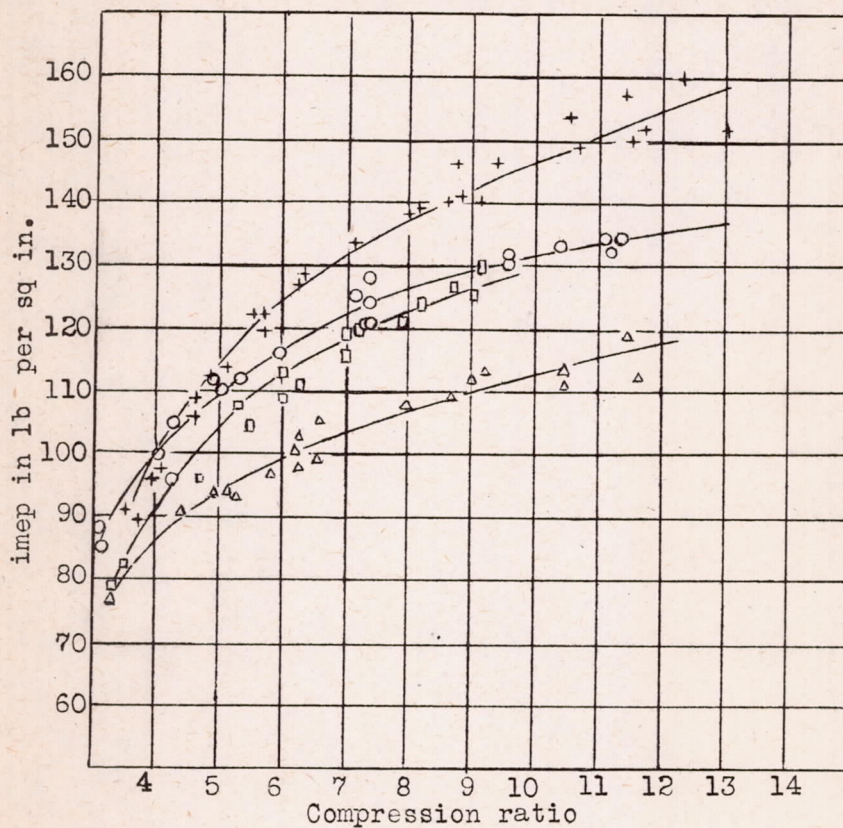


Figure 33.- Indicated mean effective pressure vs. compression ratio for four standard conditions (reference 14).